

Fortgeschrittenes Physikalisches Praktikum

Wintersemester 24/25

Versuch F96

Tutor: Julia Ines Jaeger

Characterisation of Silicon Pixel Sensors

In this lab course, we will focus on analyzing real test-beam data from silicon pixel detectors, used in High-Energy Physics experiments, to characterize a pixel sensor prototype. The course aims to deepen our understanding of how silicon pixel detectors function and to build skills in data analysis using ROOT and Corryvreckan. We'll work step-by-step through the process, from reading raw data and conducting quality checks to performing detailed analyses on sensor performance.

1 Introduction of this experiment

1.1 Semiconductor

A semiconductor is a material that has electrical conductivity between that of a conductor and an insulator, making it essential in electronic devices. An electron-hole pair is created in a semiconductor when an electron gains enough energy to jump from the valence band to the conduction band, leaving behind a "hole" in the valence band that acts as a positive charge carrier. Doping a semiconductor involves adding impurities to the material to increase its conductivity, allowing it to have more free charge carriers, either electrons or holes, depending on the type of impurity added.

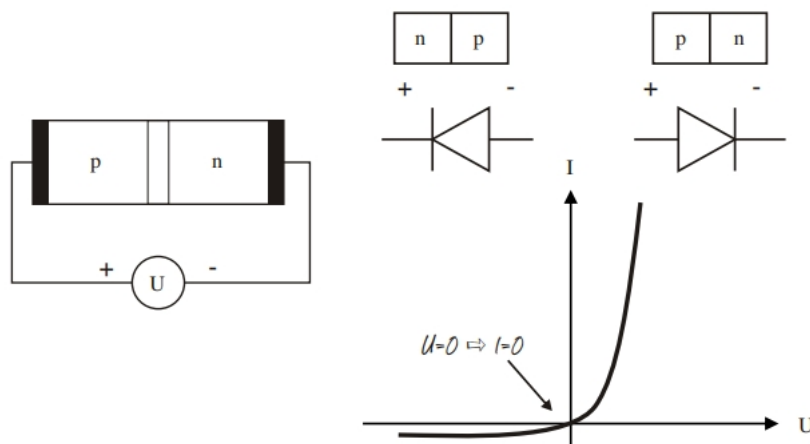


Figure 1: PN-Junction and diode

When a p-doped and n-doped semiconductor are brought into contact, they form a p-n junction, where electrons and holes diffuse into the opposite sides, creating a built-in electric field that opposes further charge movement, forming the basis for diodes.

The depletion region is the area around the p-n junction where mobile charge carriers are depleted due to recombination, leaving behind charged ions and creating an electric field that opposes further charge diffusion.

When a voltage is applied across a diode, the behavior depends on the direction: in forward bias, current flows easily; in reverse bias, only a very small current flows until breakdown voltage is reached. Forward bias occurs when the p-side of the diode is connected to a positive voltage, reducing the depletion region and allowing current flow, whereas reverse bias connects the n-side to positive voltage, widening the depletion region and preventing current flow.

1.2 Ionization

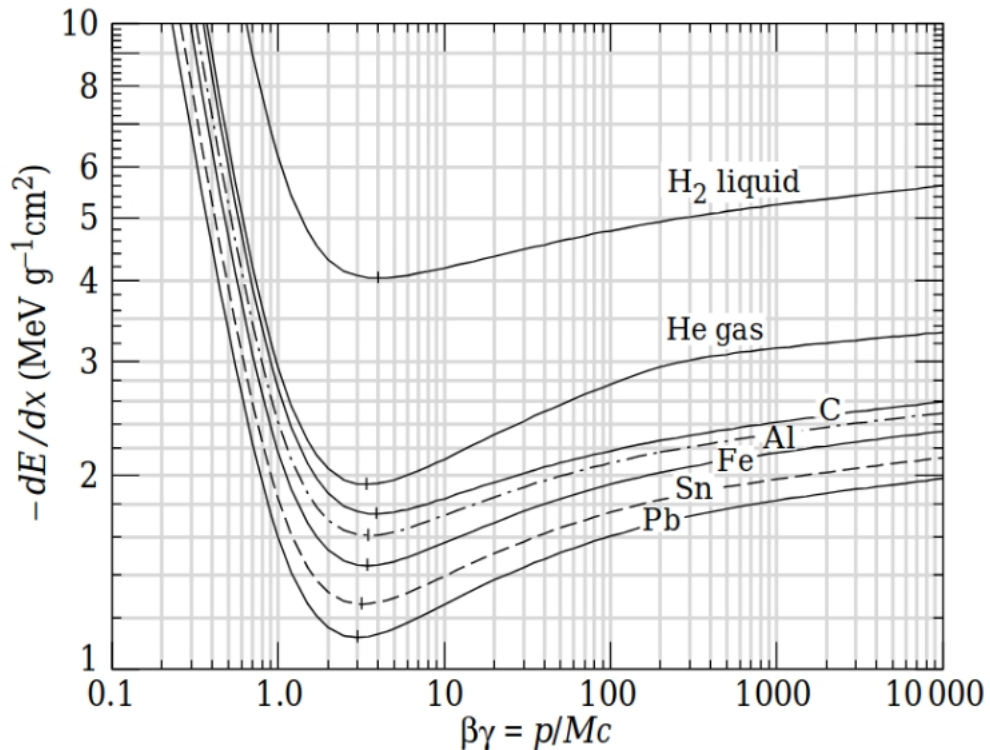


Figure 2: Bethe-Bloch-curve

Ionization is the process of removing electrons from atoms or molecules, creating ions. In semiconductors, ionization generates electron-hole pairs that contribute to conductivity.

The Bethe-Bloch formula describes the energy loss per unit path length of a charged particle traveling through matter, mainly due to ionization and excitation of atoms in the medium. For the Minimum-ionizing particles are those that lose the least amount of energy per unit distance as they travel through a material, commonly observed near the speed of light.

1.3 Silicon pixel sensors

In a pixel sensor, a signal is generated when a charged particle passes through the silicon, creating electron-hole pairs along its path due to ionization. If these electron-hole pairs are within the depletion region of the reverse-biased pn-junction, they are separated by the electric field and drift toward the collection electrodes. As the charges drift, they induce a signal on the collection electrodes, which can be amplified and processed as an electrical signal to register the particle's presence.

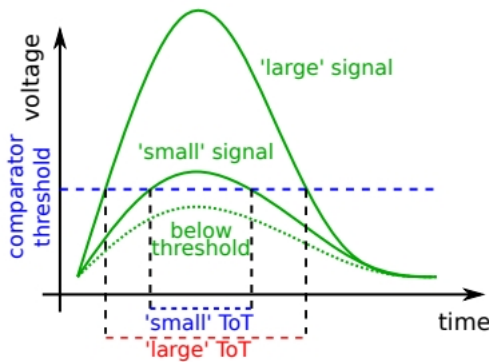


Figure 4: Illustration of the detection threshold and the **time-over-threshold (ToT)** measurement for different pulse heights.

Figure 3: Illustration of ToT

Reference: Jens Kröger, script F96 silicon pixel sensor P.6

ToT (Time-over-Threshold) measurement represents the time that the amplified signal stays above a certain threshold level. This duration correlates with the amount of charge deposited by the particle. By using an energy calibration, the ToT value can be translated into the actual charge deposited, where a large ToT indicates a large deposited energy, and a small ToT indicates a smaller deposited energy.

The spectrum of energy loss of ionizing particles in thin layers, often follows a Landau distribution, where most particles lose energy in a narrow range, but there are occasional higher losses, creating a long tail in the distribution. This correlates with the ToT measurement, as the distribution of ToT values reflects the energy deposited by the ionizing particles in the sensor material.

Noise in the sensor can cause false or "fake hits" that mimic actual particle detections. Noise may be caused by thermal fluctuations in the amplifier's output signal, instability in the threshold settings, or external factors like poor solder connections or other hardware issues.

1.4 Types of sensors

The difference between **hybrid** and **monolithic** detectors lies in their structure.

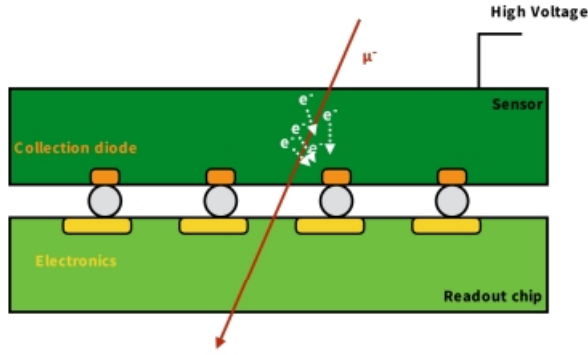


Figure 4: Hybrid pixel sensor

Reference: Jens Kröger, script F96 silicon pixel sensor P.6

Hybrid detectors have two separate layers: the sensor layer (for detecting particles) and the readout chip (containing amplifiers, discriminators, and other electronics), connected via bump-bonds. Hybrid detectors offer the advantage of greater flexibility, as they allow for combining specialized sensor and readout materials, making them suitable for high-radiation environments where they maintain performance over time. However, they are more complex to manufacture due to the bump-bonding process, and they tend to be more costly.

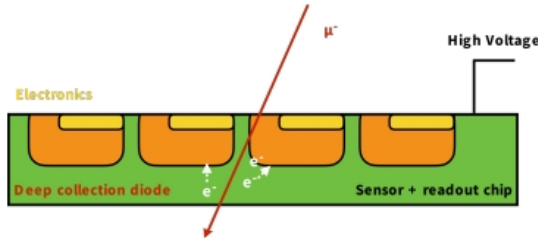


Figure 5: Monolithic pixel sensor

Reference: Jens Kröger, script F96 silicon pixel sensor P.6

Monolithic detectors combine the sensor and readout electronics in a single silicon layer, with signal processing integrated within each pixel. So monolithic detectors are simpler and more compact, integrating detection and readout electronics in a single layer, which makes them cheaper, lighter, and capable of faster charge collection, especially in high-voltage MAPS (HVMAPS), improving timing and resolution. Their main drawbacks are limited material choices and reduced radiation hardness, which can shorten their lifespan in high-radiation settings compared to hybrid detectors.

1.5 Experimental setup and Test-beam reconstruction Chain

In this experiment the particles were shot through the Timepix3 telescope with a device-under-test (DUT).

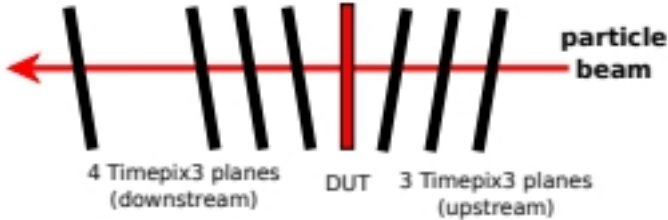


Figure 6: Timepix3 telescope with a device-under-test (DUT) at the SPS, CERN.
Reference: Jens Kröger, script F96 silicon pixel sensor P.9

The Test-beam Reconstruction Chain processes test-beam data to characterize pixel sensors.

- It starts by **reading raw binary data**, extracting pixel hit details like position, timestamp, and charge.
- A **Clustering** algorithms groups neighboring pixel hits then, adapting charge sharing to improve spatial resolution.
- Before the tracking there are **correlations** and **alignment**, correlations are then calculated for initial data checks, ensuring spatial coherence; and the alignment will be conducted to achieve accurate tracking, as it refines detector positions and rotations beyond manual measurements.
- Afterwards **Tracking** combines clusters from various telescope planes to form straight-line tracks, but excluding DUT to avoid bias.
- Next, the DUT is **associated with reference tracks** for comparison.

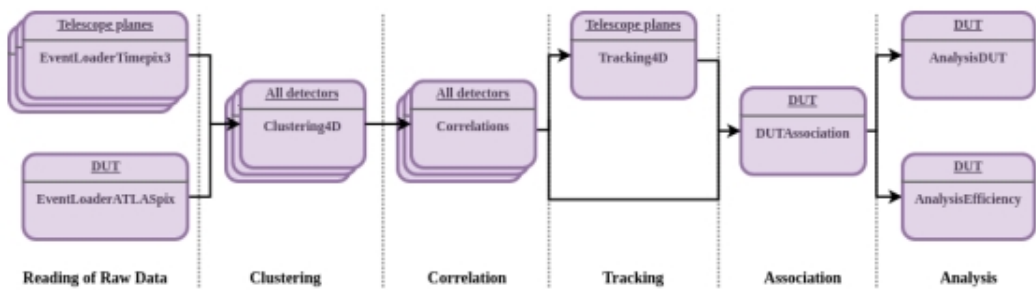


Figure 7: Test-beam reconstruction chain
Reference: Jens Kröger, script F96 silicon pixel sensor P.12

2 Execution

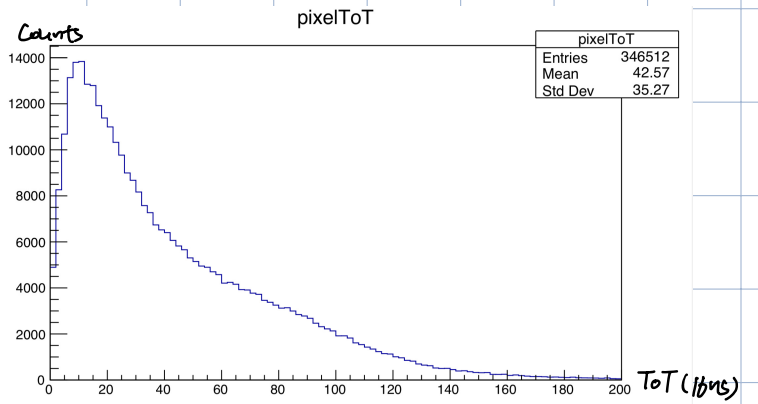
Macros can be found under <https://heibox.uni-heidelberg.de/d/de7f3d9c832d4a9c8ee8/>

F96 Characterisation of Silicon Pixel Sensors

01. 11. 2024

Group: Yulai Shi Yuting Shi

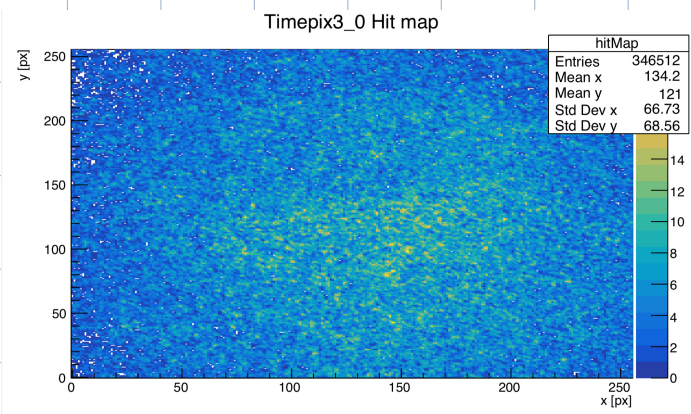
Open the example data files



ToT distribution

ToT \approx energy of electrons

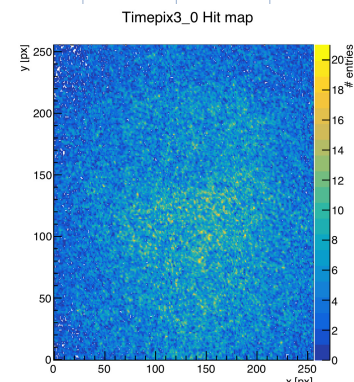
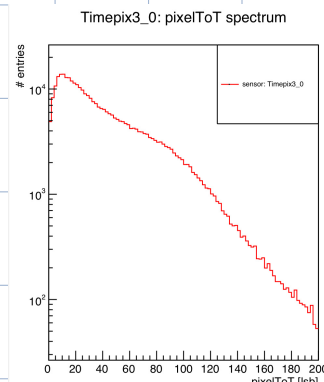
particles loss energy and create e^- - e^+ pairs. The long tail occurs because occasionally particles transfer a large amount of energy in a single collision.



2D - Hitmap

Std. Dev. of x,y same ($66 \approx 68$),
 \Rightarrow circular beam cross section

Open example-macro.C



ConfigureScan

Open configuration file:

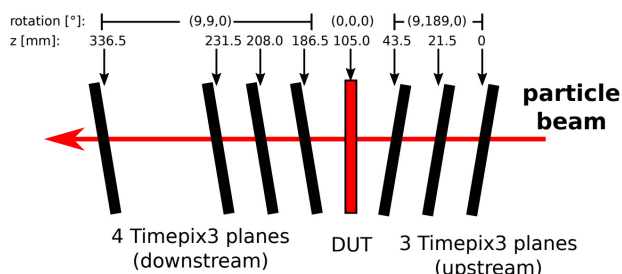
- The configuration file specifies the detector and histogram files to be used. The main configuration file specifies the reconstruction chain by listing modules and parameters, with defaults applied if not specified.
- The detector file, with a `.geo` extension, defines the detector geometry and can be considered as our initial conditions.
- The histogram file, a `root` file, contains previously analyzed measurements from the detector and is an output file.
- There is a "Metronome" setting that sets a fixed time interval of 20 μ s for sequential processing to manage large datasets efficiently.
- Modules like EventLoaderTimepix3 and Clustering4D operate event-by-event, and the output ROOT file is saved when analysis completes or is interrupted.

Open .geo Data file : This file contains the information about detector type, size, resolution and orientation

Run the ConfigureScan - example script: The files are missing from which the hit data is obtained. The output result of example.root has already been observed at the beginning

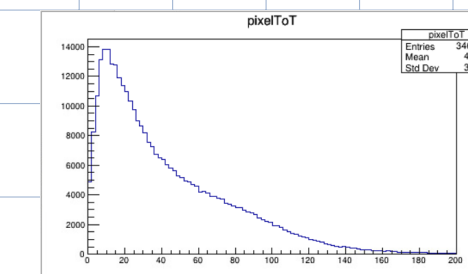
4.2 Reading in the Raw Data

We complete the geometry file 02-read-data.geo at first.

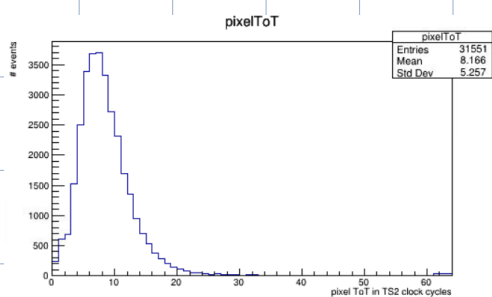


Output in Root

Timepix 3



Atlas



→ Macro

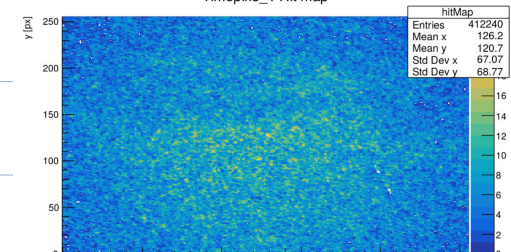
Geometrical information

The resolution of ATLASpix-simple is assumed as a binary resolution.

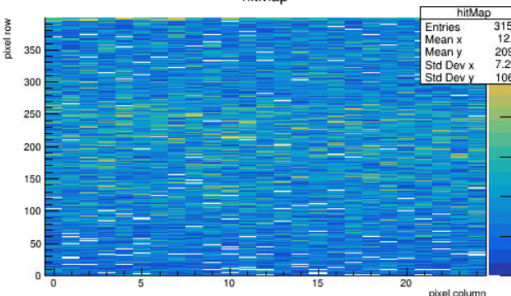
$$\text{RMS binary } x/y = \frac{\text{Pixel pitch in } x/y}{\sqrt{2}}$$

$\sqrt{2}$

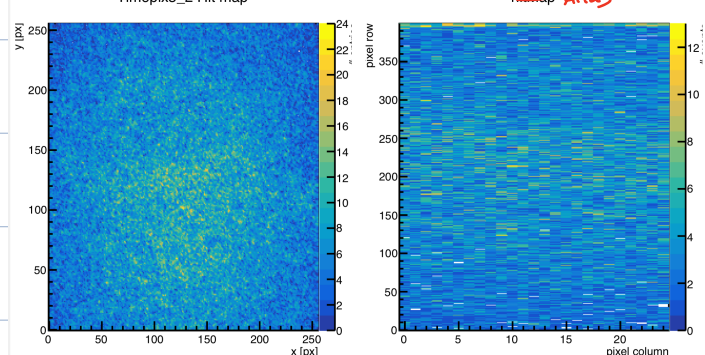
Timepix3_1 Hit map



hitMap

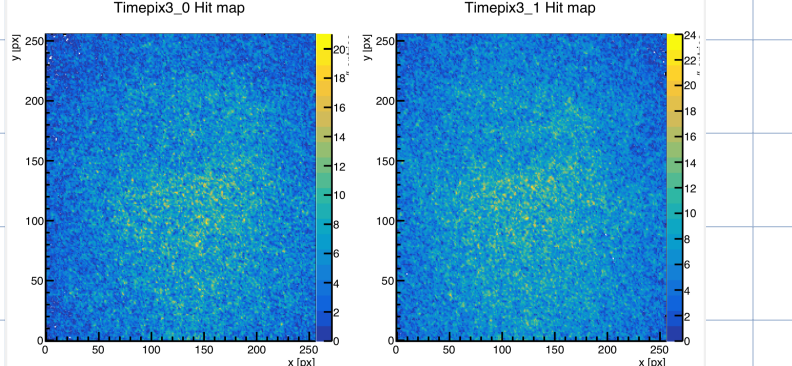


Timepix3_2 Hit map

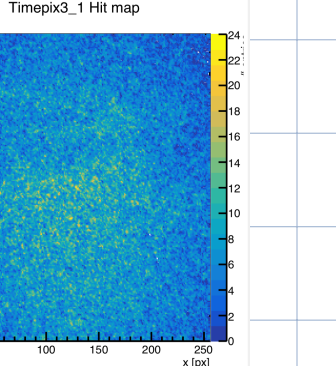


hitMap Atlas

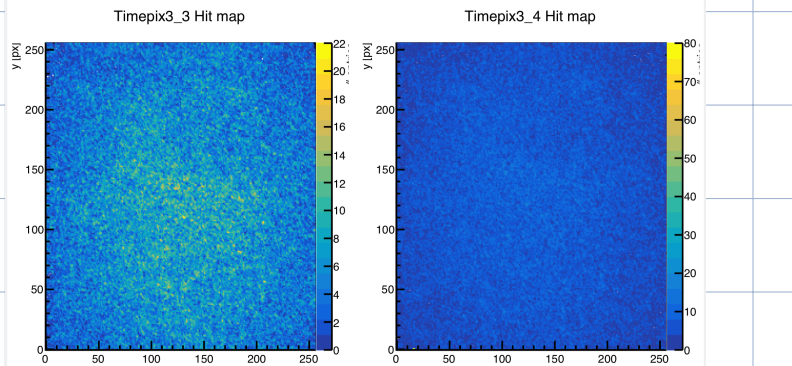
Timepix3_0 Hit map



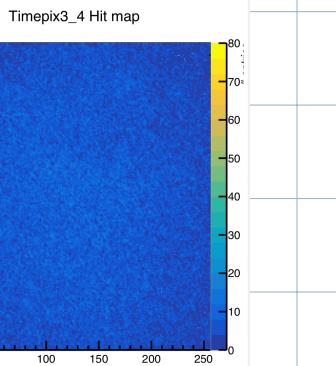
Timepix3_1 Hit map



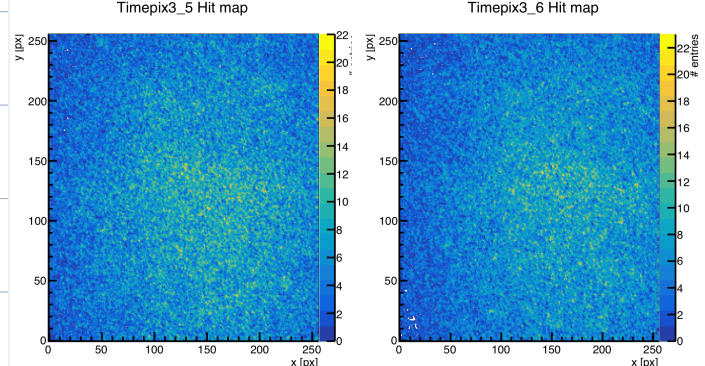
Timepix3_3 Hit map



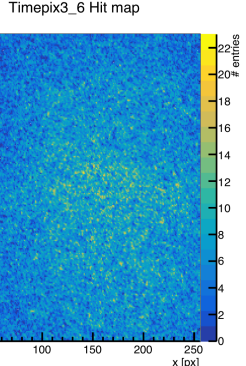
Timepix3_4 Hit map



Timepix3_5 Hit map



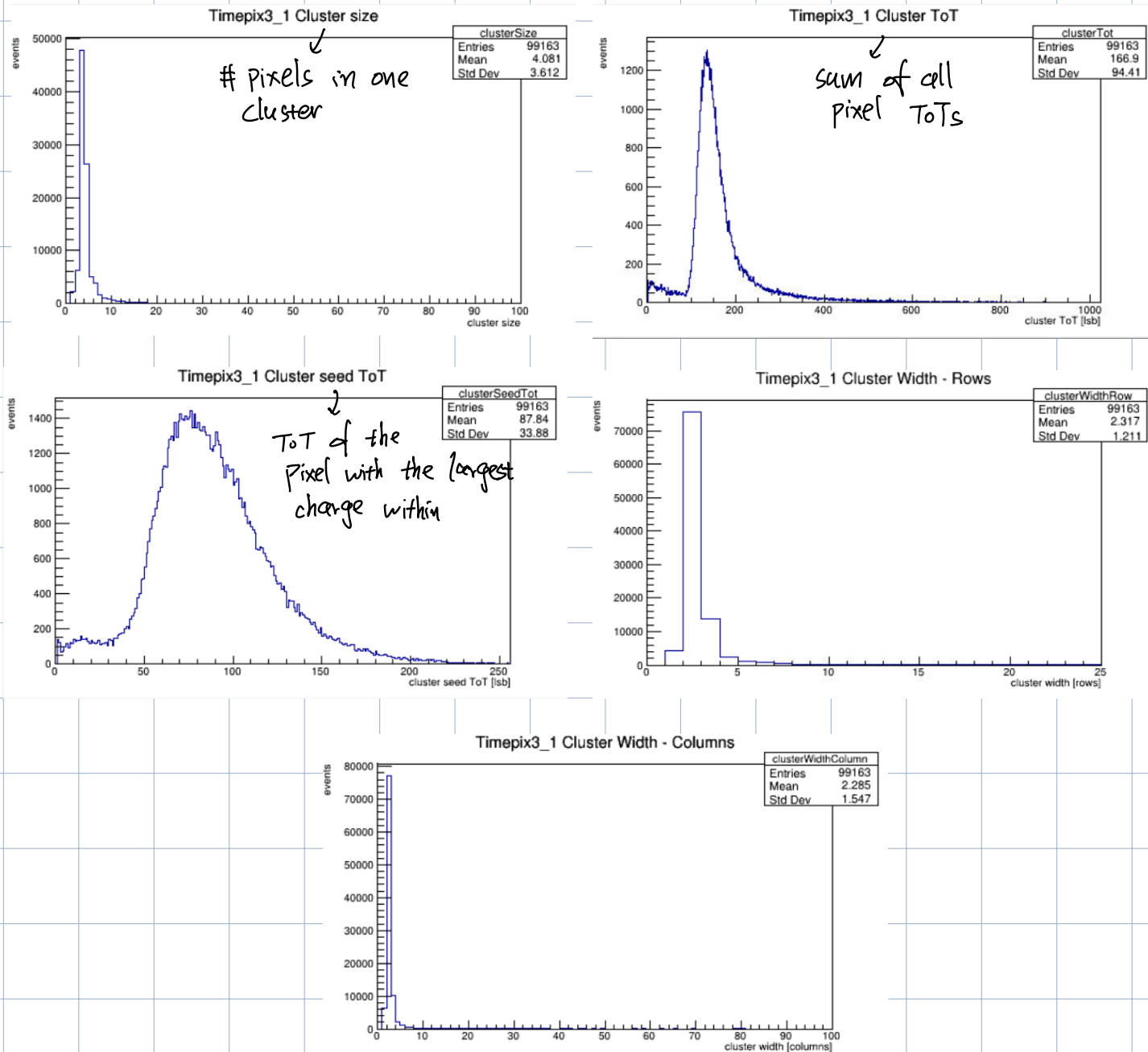
Timepix3_6 Hit map



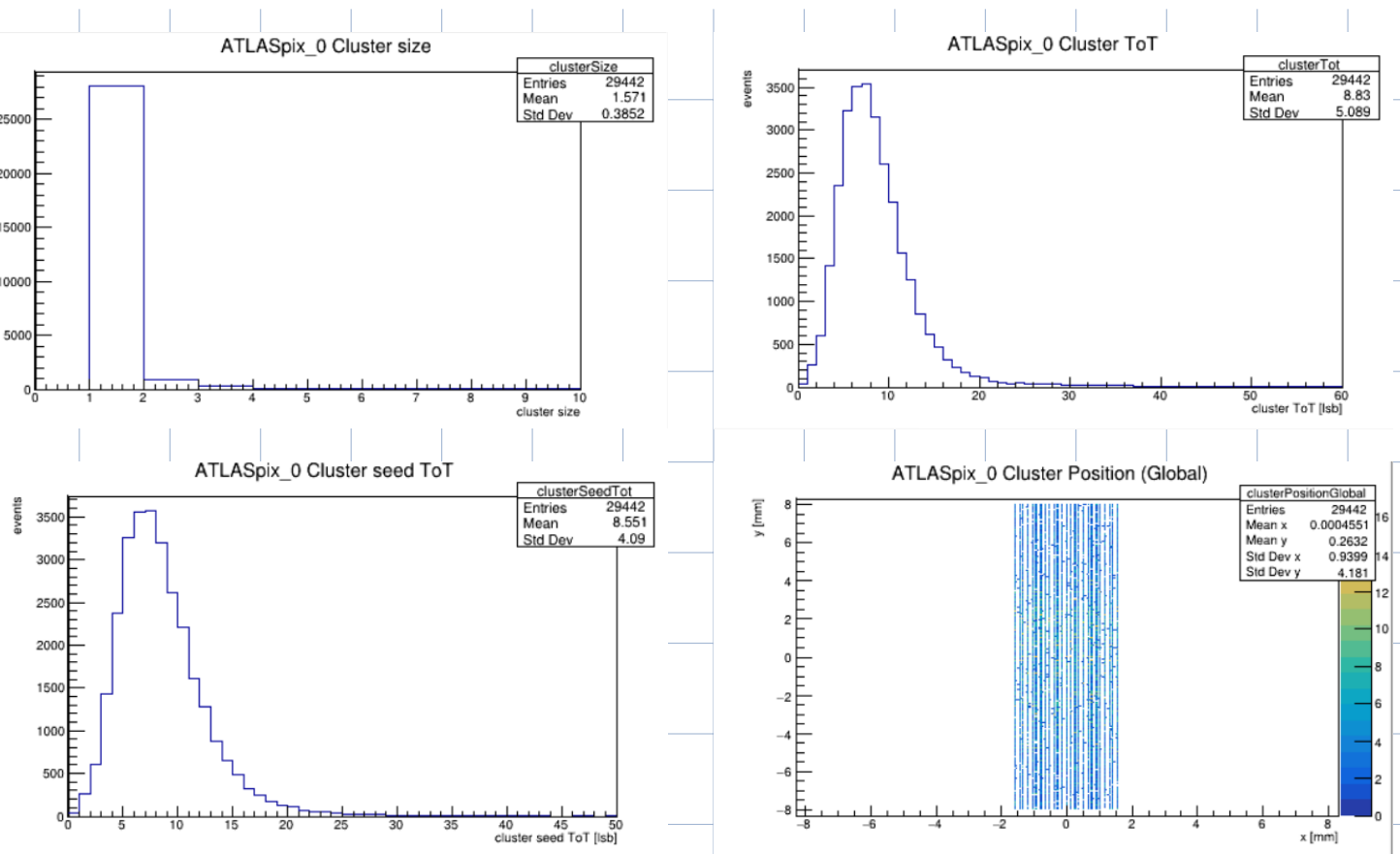
The hit map of the Atlas detector contains many pixels like rectangles, this may be due to the different resolution in comparison with other telescopes. The hit maps for the detector planes show a generally similar distribution of events across the pixel area, but Timepix3_4 stands out with a significantly higher event density, reaching around 80 entries, compared to other planes that max out around 20. This discrepancy could stem from its positioning within the telescope, variations in sensor efficiency, or environmental factors like background radiation or orientation.

4.3 Clustering

Timepix3 :



Atlas :



Write macros to draw the overlap plots:

- **Cluster Sizes for Timepix3 vs. ATLASpix_Simple:**

The cluster size distribution for `Timepix3_0` has a larger range of cluster sizes, while `ATLASpix_0` appears to have smaller clusters on average. This difference could be due to sensor architecture. Timepix3 have a finer spatial resolution, resulting in larger cluster sizes as more pixels are included in a cluster. ATLASpix, designed differently, might group fewer pixels, yielding smaller clusters. (The resolutions can be found in the geometrical data file.)

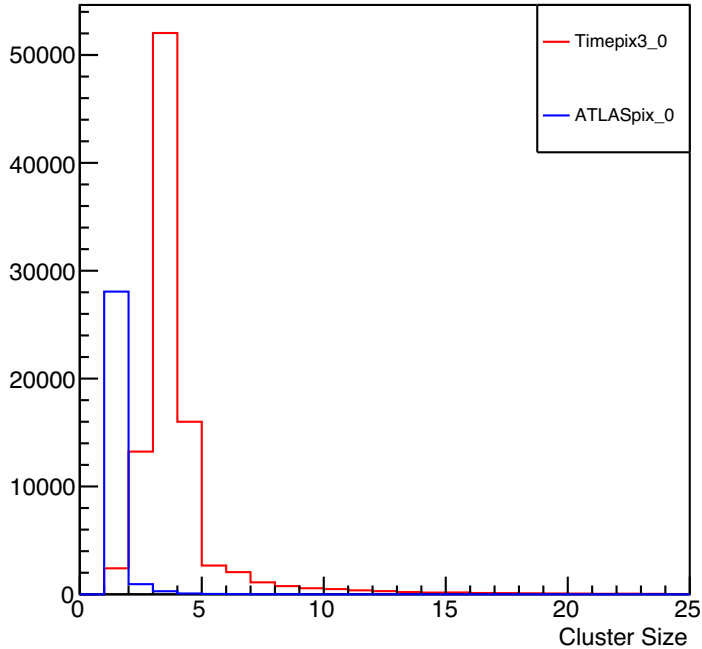
- **Cluster Width in Column and Row for ATLASpix_Simple:**

The distribution shows that the `clusterWidthColumn` and `clusterWidthRow` for ATLASpix are similar but not identical, with a slightly broader distribution for row depending on pixel configuration. This difference might arise from the sensor's layout. If the sensor's geometry or readout mechanism favors one direction, clusters could be elongated along that axis. Environmental factors, like the angle of particle hits, could also impact width measurements.

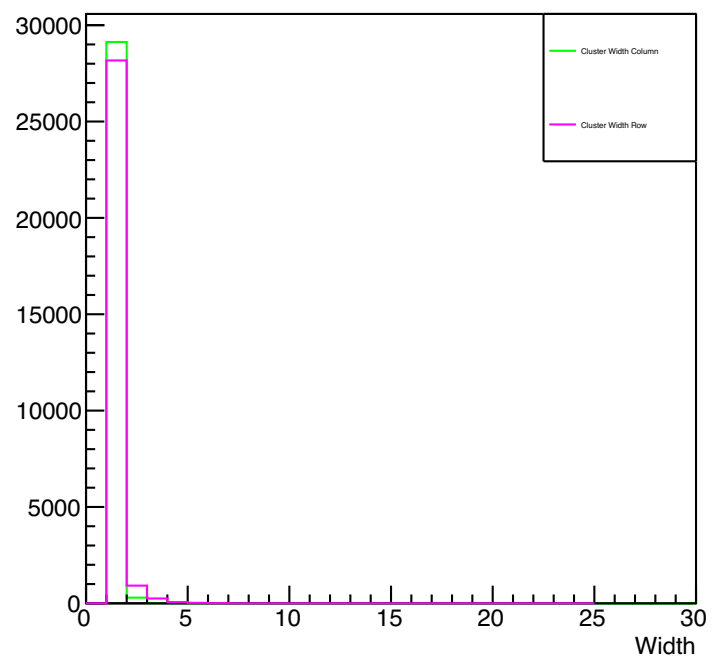
- **Seed Pixel ToT and Cluster ToT for ATLASpix_Simple vs. Timepix3:**

The peak of ATLASpix in both diagrams about ToT is significantly higher than Timepix3. However, Timepix3 shows a broader distribution in `Cluster Tot`, suggesting it records higher cumulative signals. This difference could stem from sensor sensitivity and design. Timepix3, possibly more sensitive, captures a higher total signal, resulting in a more spread-out `Cluster Tot`. ATLASpix, designed for a different purpose or particle type, may prioritize capturing peak signals at the seed pixel rather than the total across the cluster

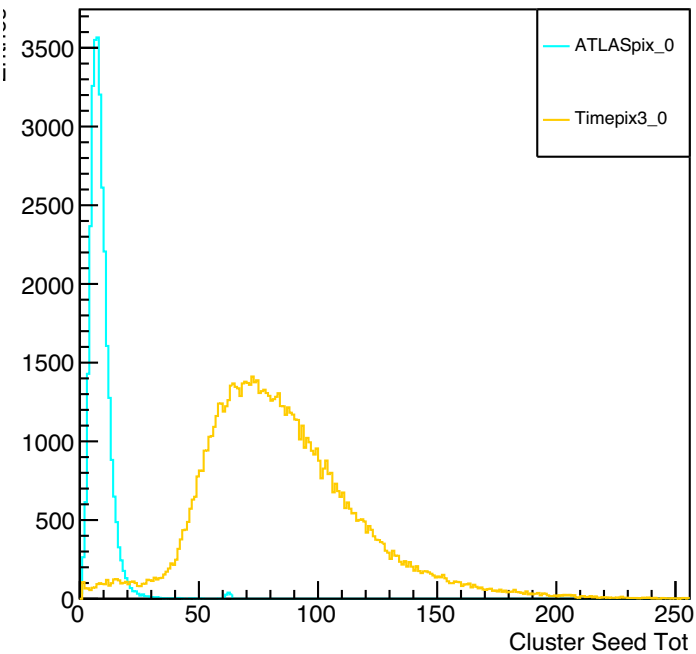
Timepix3_0/ATLASpix Cluster Size Comparison



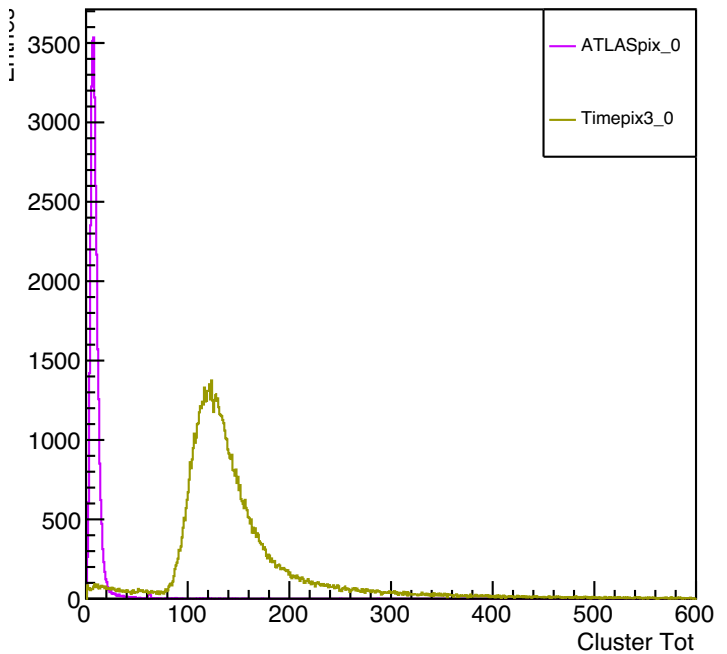
Cluster Width for ATLASpix



Cluster Seed Tot Comparison



Cluster Tot Comparison

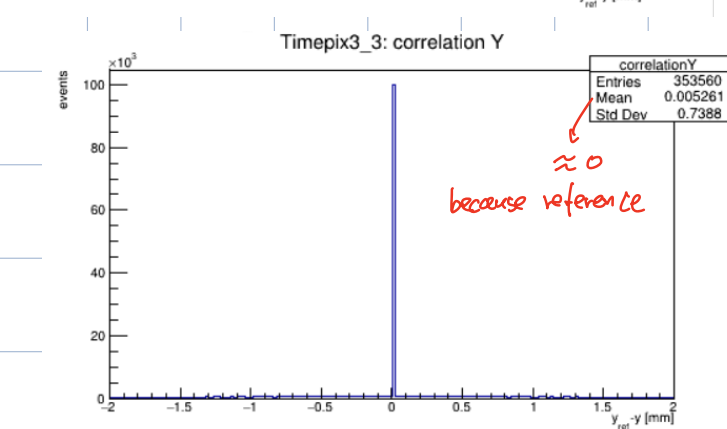
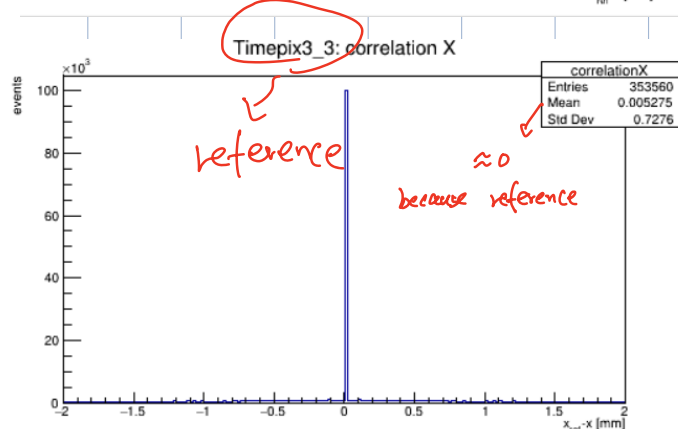
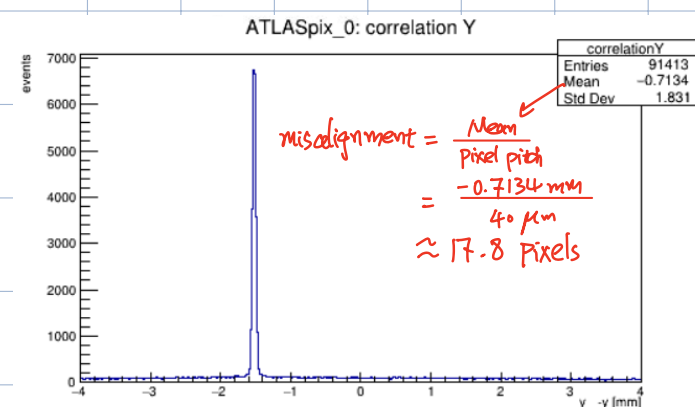
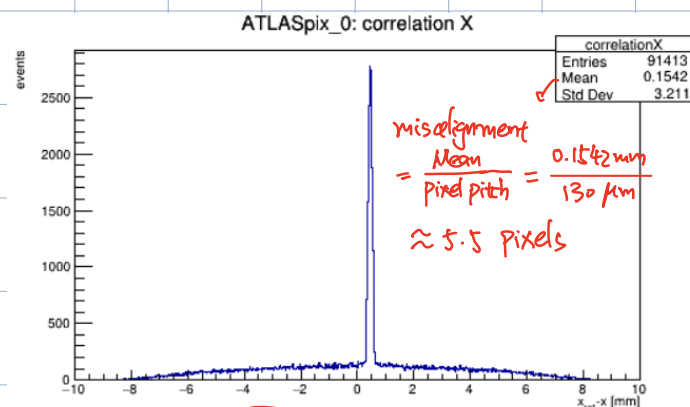
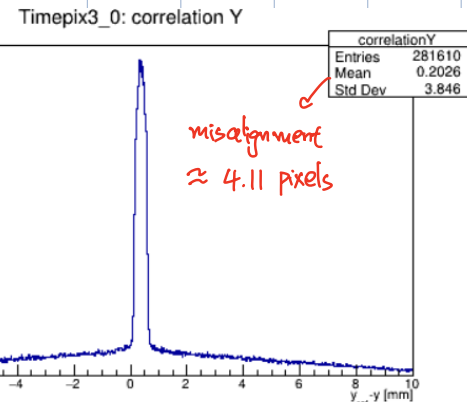
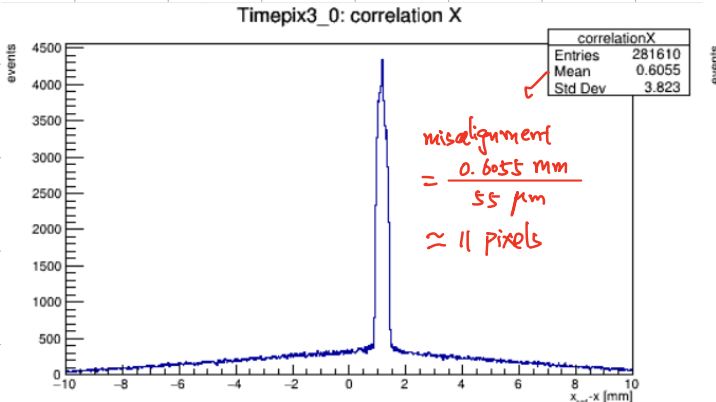


4.4 Correlations: We run the main configuration file `04-correlations-telescope.conf`.

$$X \text{ correlation} = X_{\text{cluster on reference detector}} - X_{\text{cluster on this detector}}$$

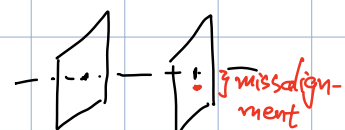
Timepix3_3

$$Y \text{ correlation} = Y_{\text{cluster on reference detector}} - Y_{\text{cluster on this detector}}$$



- Translational misalignments are visible as shifts in the peaks of the correlation histograms. Since we assume that $x, y = 0$ for all detectors, so ideally the correlation histograms should peak around zero, meaning clusters from both detectors align spatially.

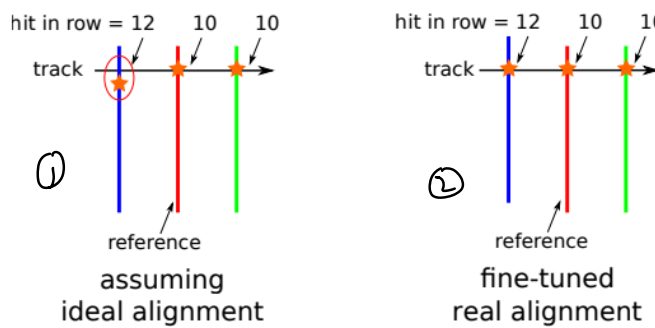
- Rotational misalignments cause the peaks in the correlation plots to spread out or tilt, rather than a sharp peak around zero.
⇒ peaks would likely show broader or asymmetrical distributions.



Until now: No tracking is involved.

4.5 Alignment and Tracting

Task: The alignment procedure in x- and y-positions and the rotation must be conducted to increase the tracking quality.



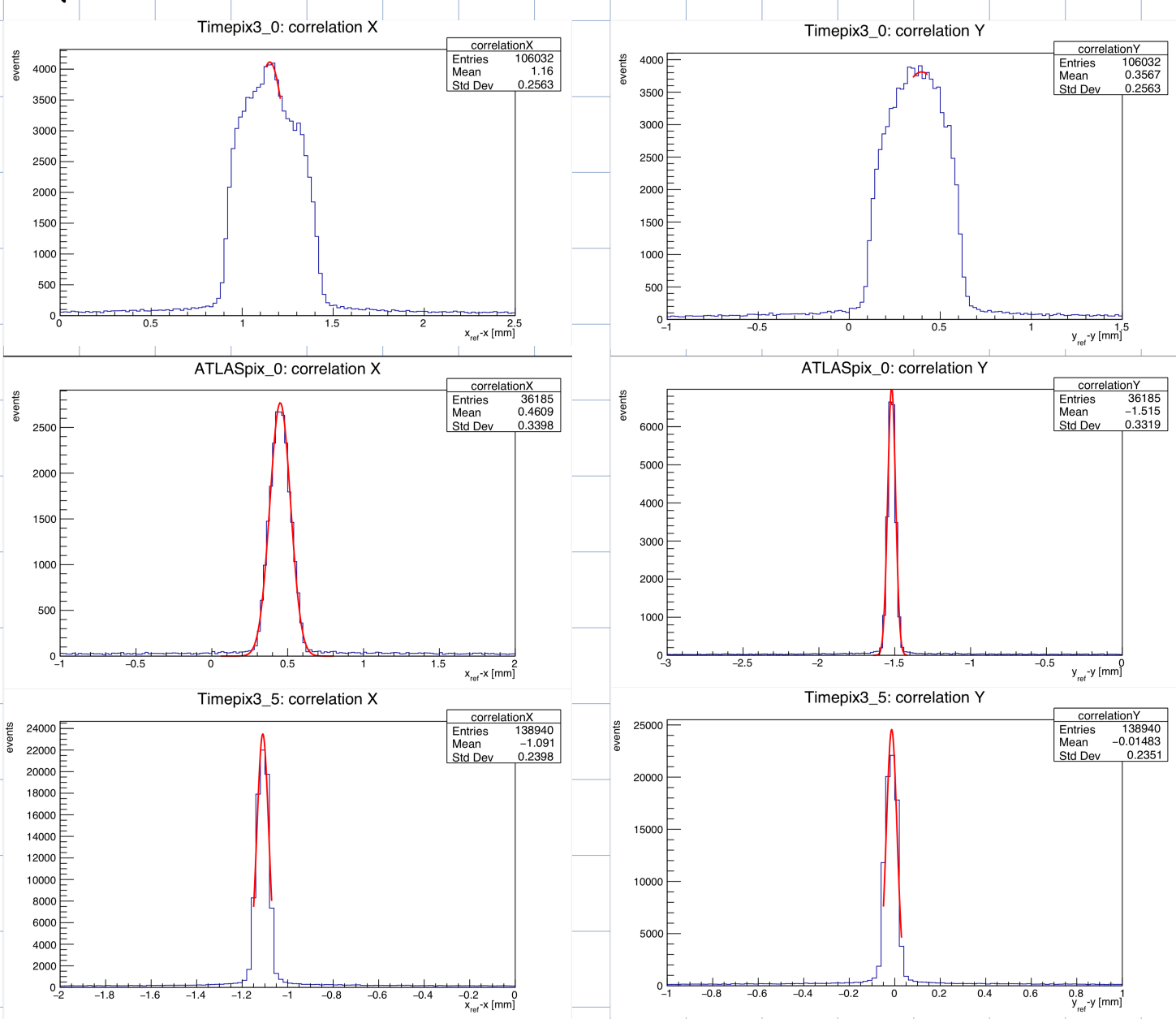
before: ①, unbiased alignment

now: ②, biased alignment

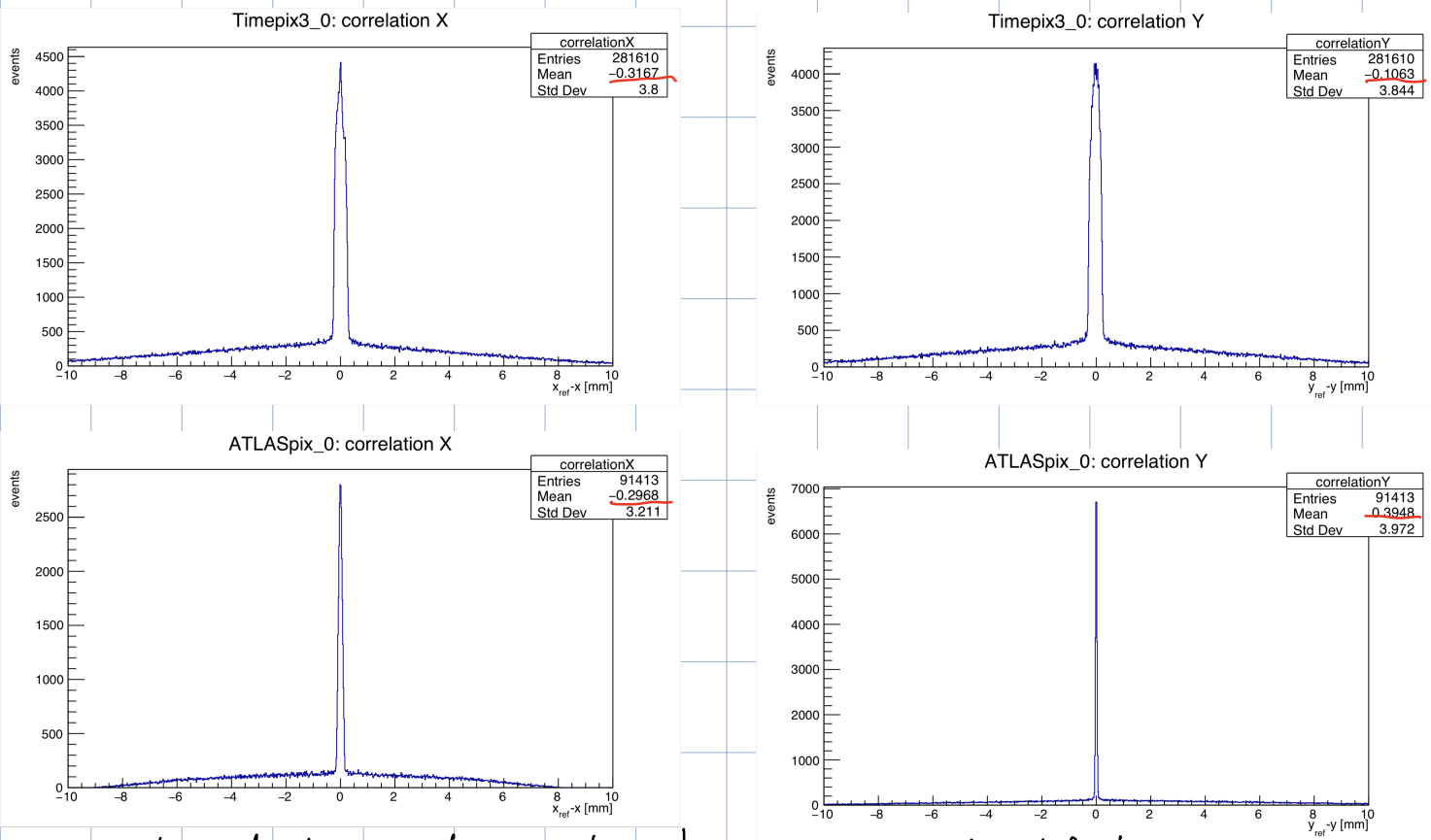
=> force the residual to be centered around zero

4.5.1 Prealignment

We run the configuration file 05_Prealign_telescope.conf to fit the previous correlation plots with Gauss curve, a updated geometry file will be generated after finishing the prealignment analysis..

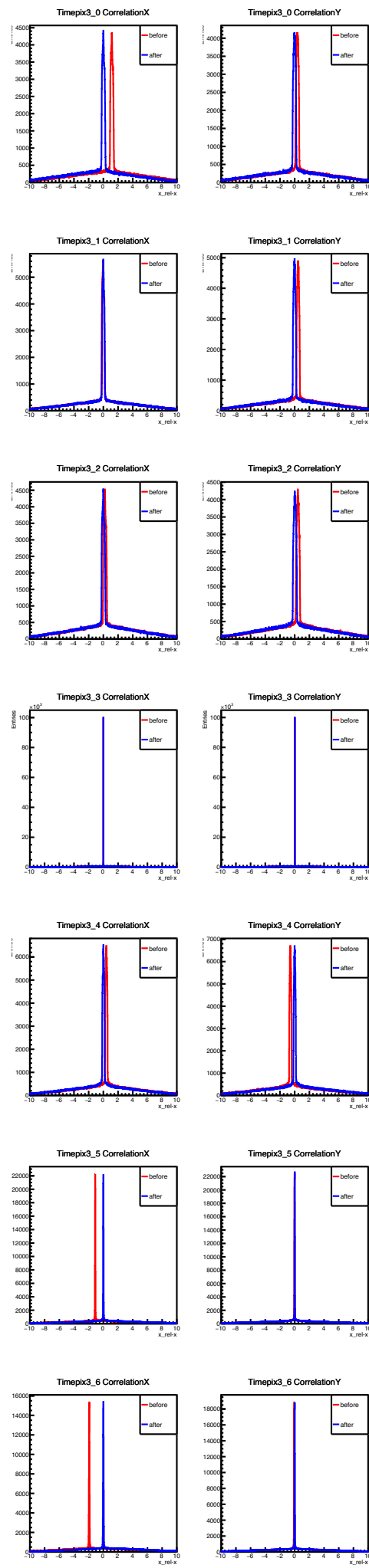


We rerun the configuration file 04-correlation.conf using the updated geometry file.



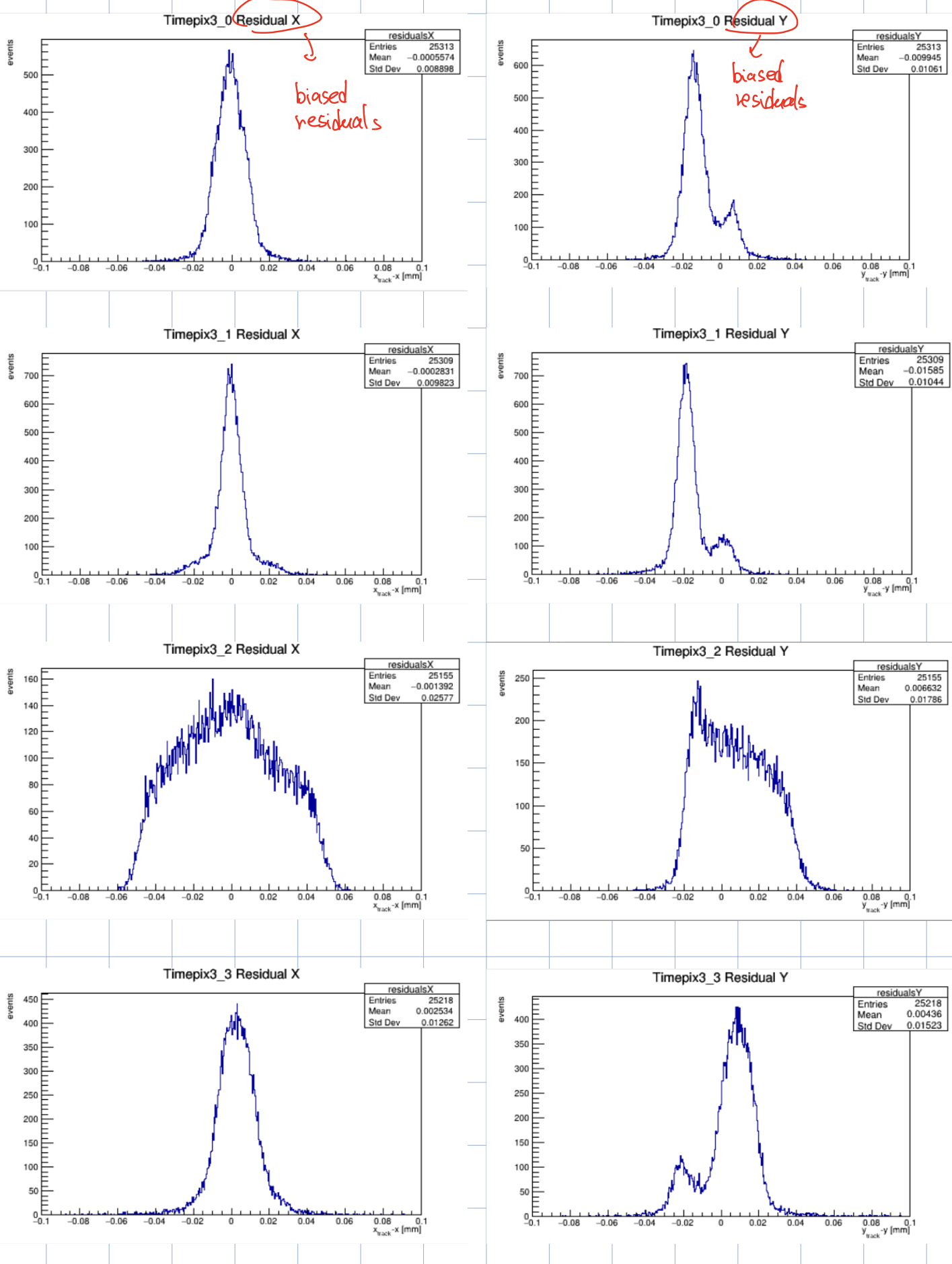
The peaks of the correlation plots have in general shifted towards zero and the mean values reduced as well.

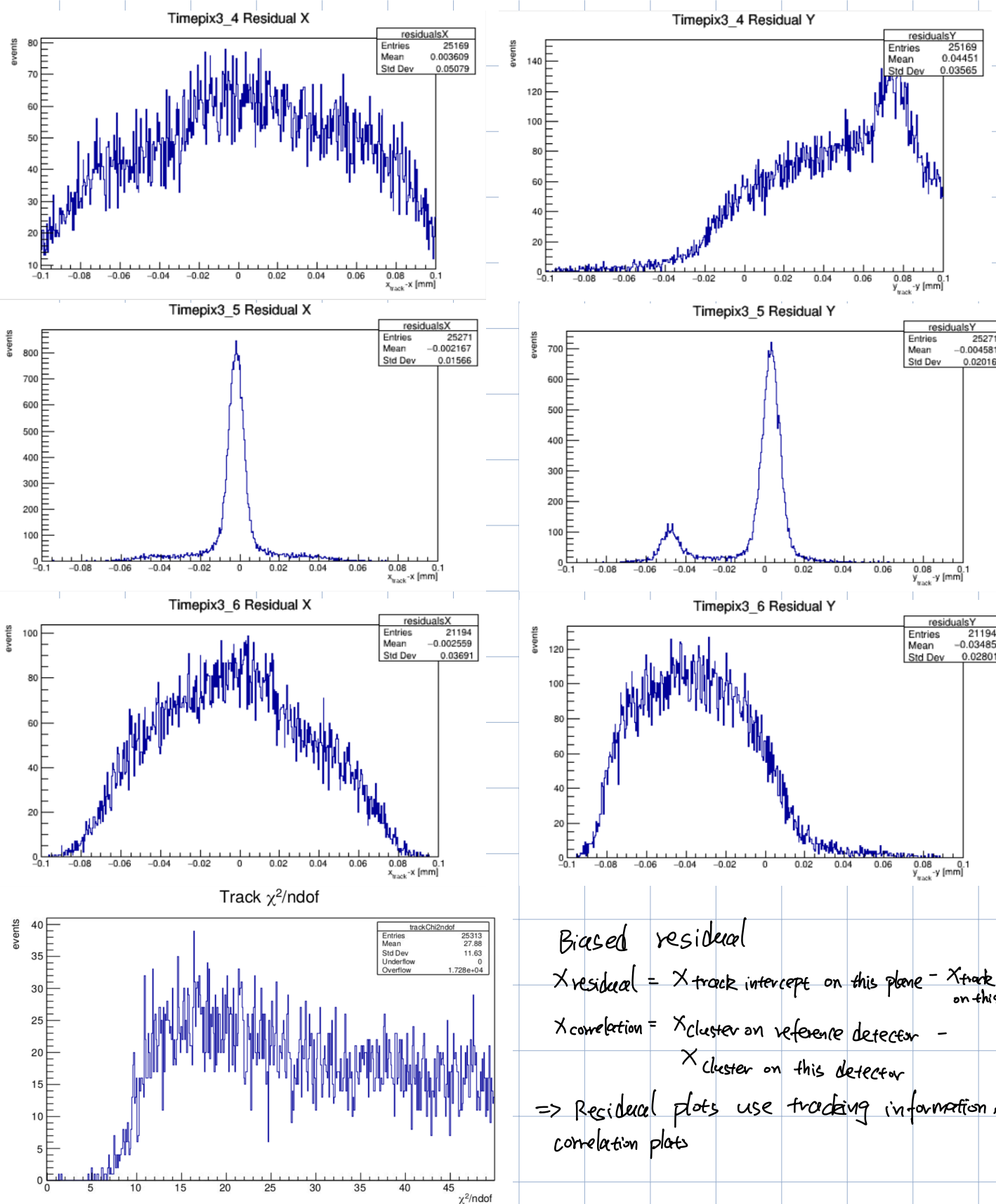
As we can see in the overlap plots of the correlations before and after, the peaks have actually been shifted.



4.5.2 First Tracking

We add module "Tracking 4D" and run the file 06-tracking.conf



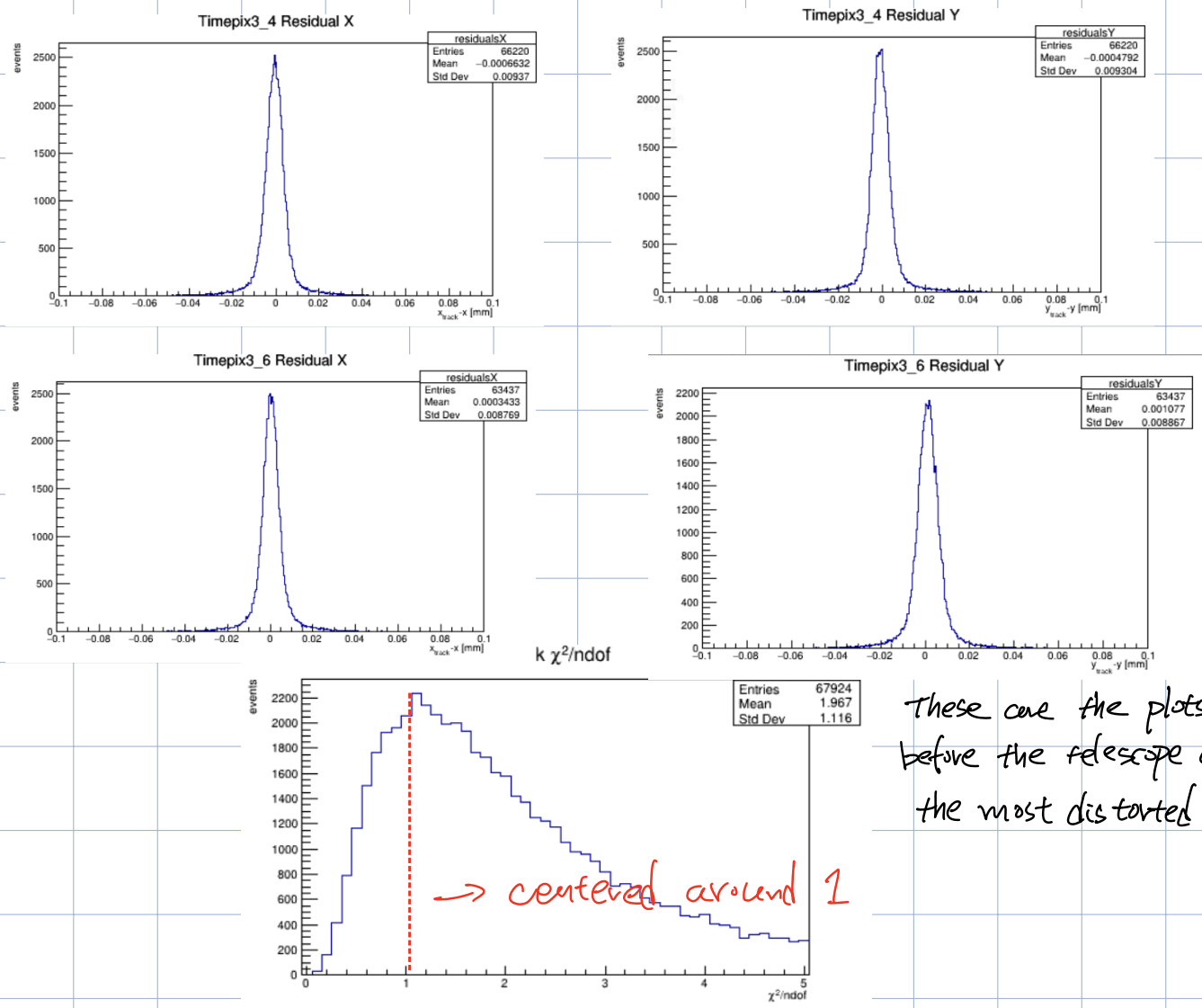


- Correlation plots are initially used to identify and approximate spatial offsets, helping correct any major misalignments in the detector setup. They allow for a visual assessment of how well detector clusters align across different layers. After prealignment, the correlation plot peaks ideally shift close to zero, forming a well-centered Gaussian shape with symmetrical distribution, indicating substantial improvement in alignment.

- However, residual plots, which assess the accuracy of alignment and tracking by showing the difference between the predicted and observed track positions on each detector layer, reveal further issues. Many residual peaks are off-center and show asymmetry or distortion, indicating that the alignment is still not optimal. Ideally, well-aligned tracks would result in residuals centered around zero in a symmetrical, Gaussian-like shape. The current residuals suggest that additional adjustments are required to achieve precise track alignment with the detectors. Further optimization will be necessary to bring the tracks closer to a fully aligned state.
- Ideally, the track χ^2/ndof should be close to 1, as this indicates a good fit between the tracks and the clusters. However, after running the tracking analysis, we inspected the χ^2/ndof values and found they were significantly higher than 1, which may suggest that there are remaining misalignments, detector noise, or other factors not accounted for in the model, the track fitting is not consistent with the detector resolution specified in the geometry file, and the alignment need to be continued.

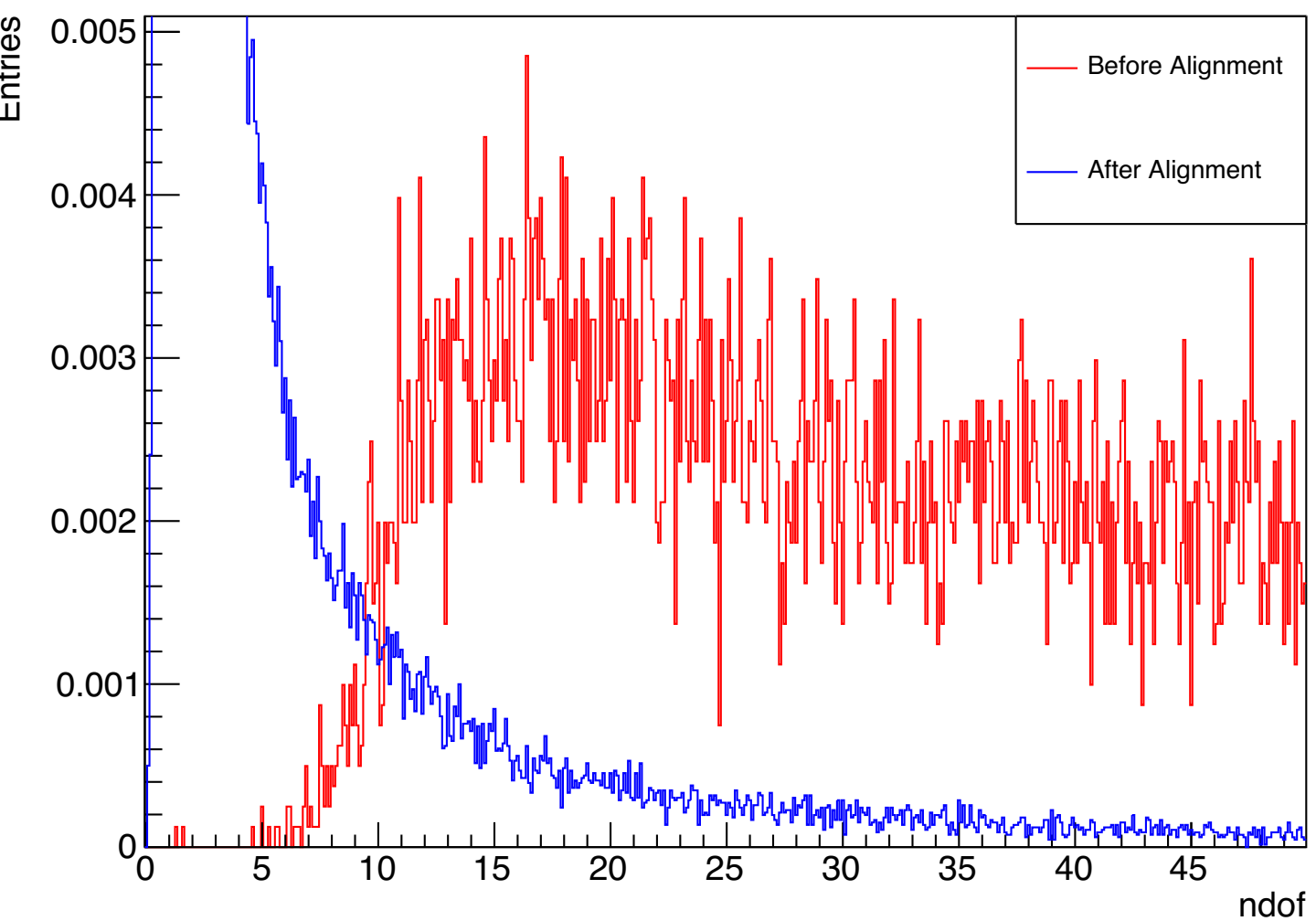
4.5.3 Telescope Alignment (Still excluding DLIT)

We run the file `07-telescope-alignment.conf` and get the new geometry file. After using the updated geometry file in `08-tracking.conf` we get the residuals and χ^2/ndof centered around 0 and 1.

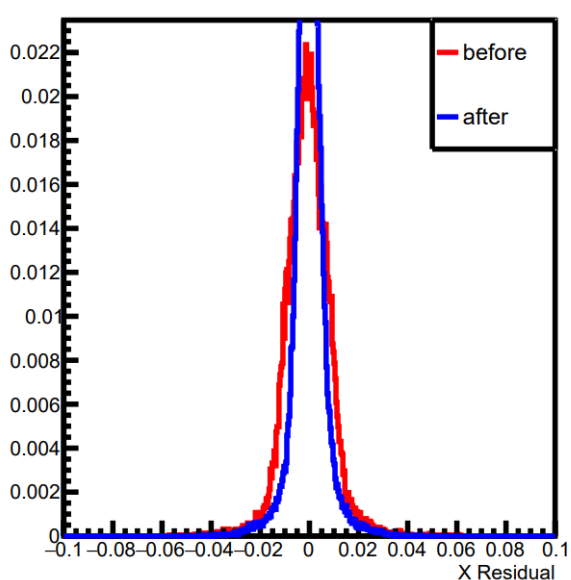


These are the plots that before the telescope alignment the most distorted.

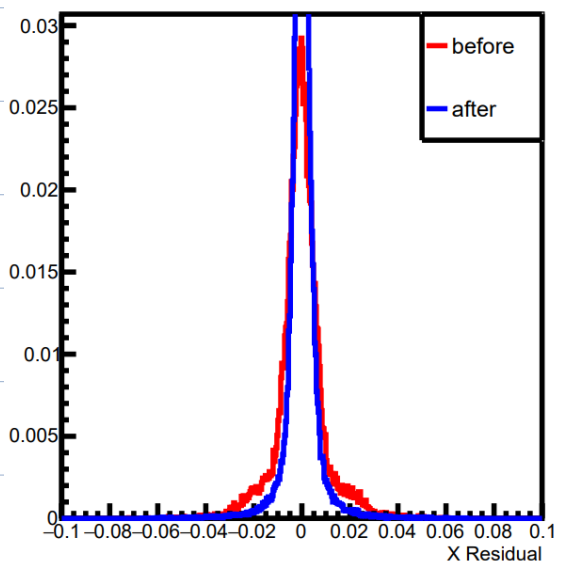
ndof Distribution Comparison



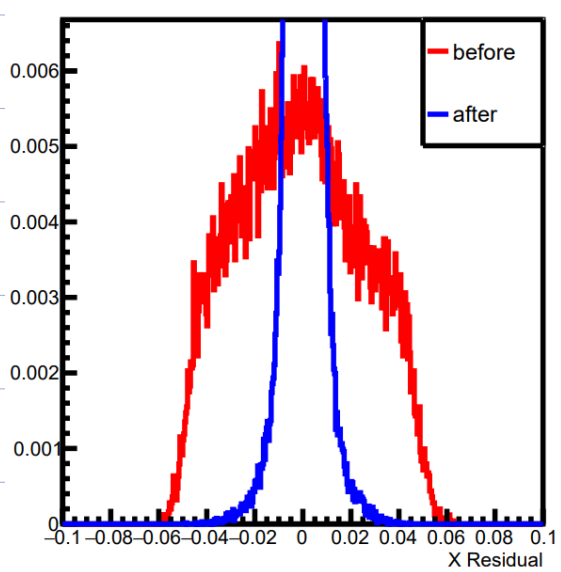
ResidualX Timepix3_0 before/after telescope Alignment



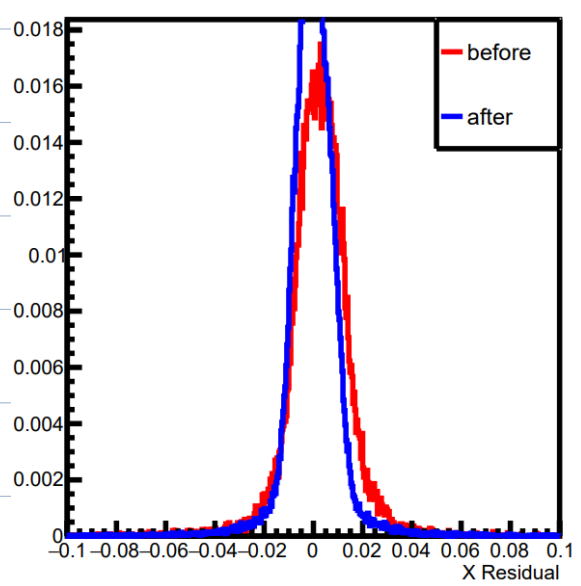
ResidualX Timepix3_1 before/after telescope Alignment



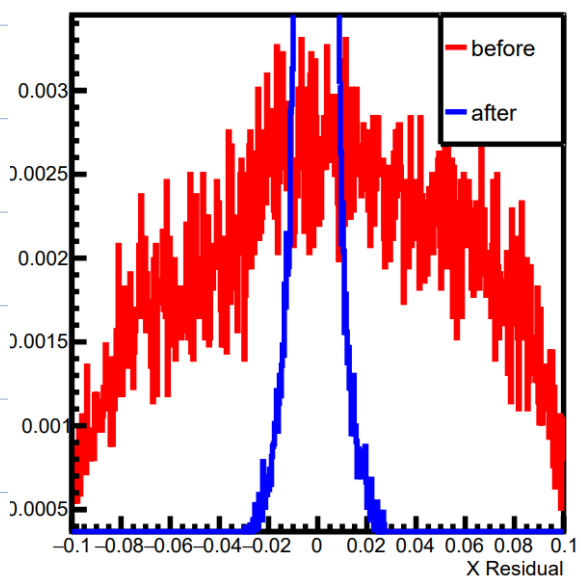
ResidualX Timepix3_2 before/after telescope Alignment



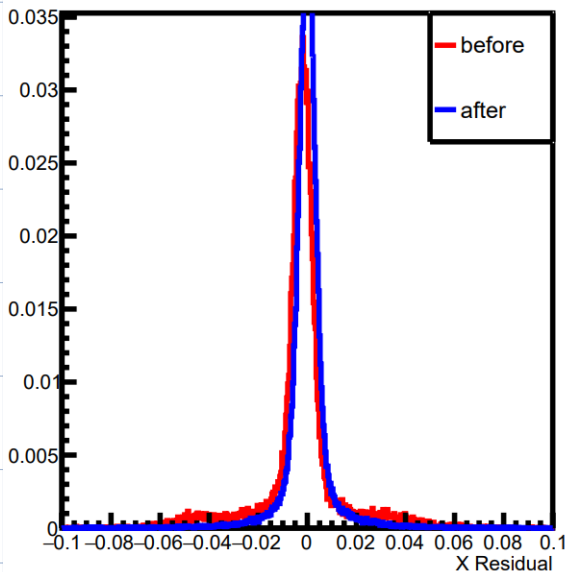
ResidualX Timepix3_3 before/after telescope Alignment



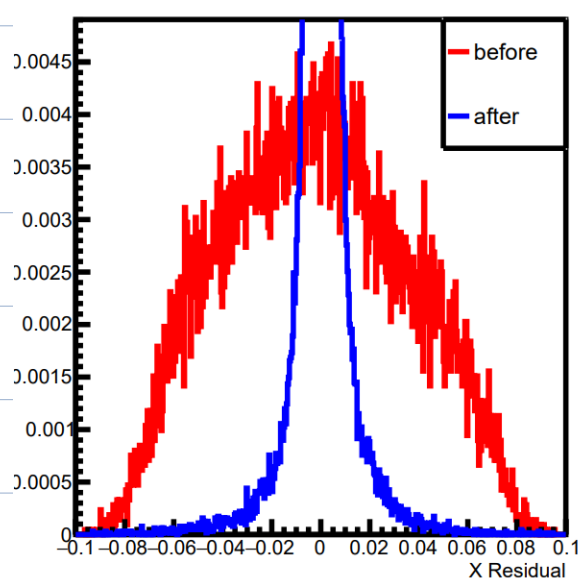
ResidualX Timepix3_4 before/after telescope Alignment



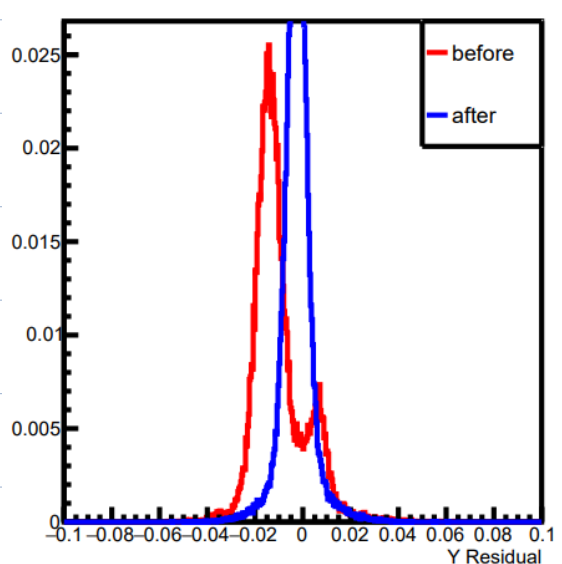
ResidualX Timepix3_5 before/after telescope Alignment



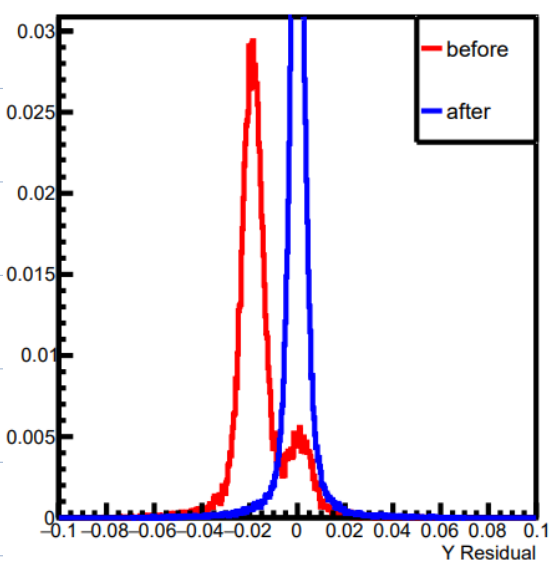
ResidualX Timepix3_6 before/after telescope Alignment



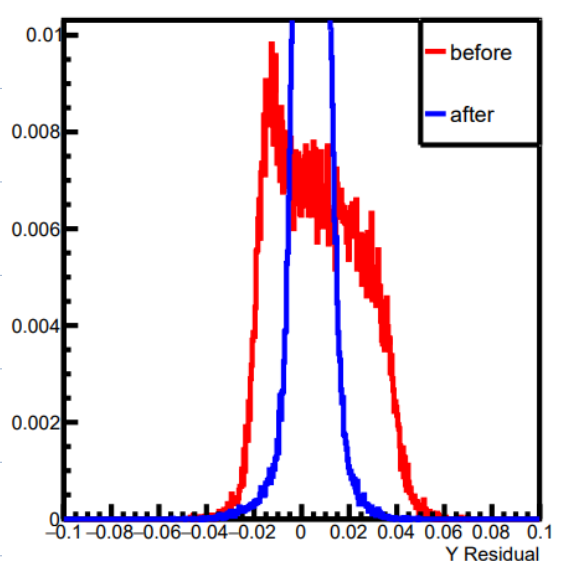
ResidualY Timepix3_0 before/after telescope Alignment



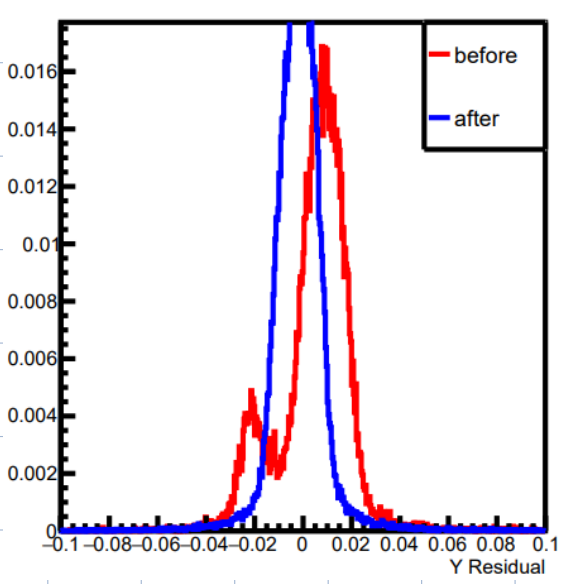
ResidualY Timepix3_1 before/after telescope Alignment



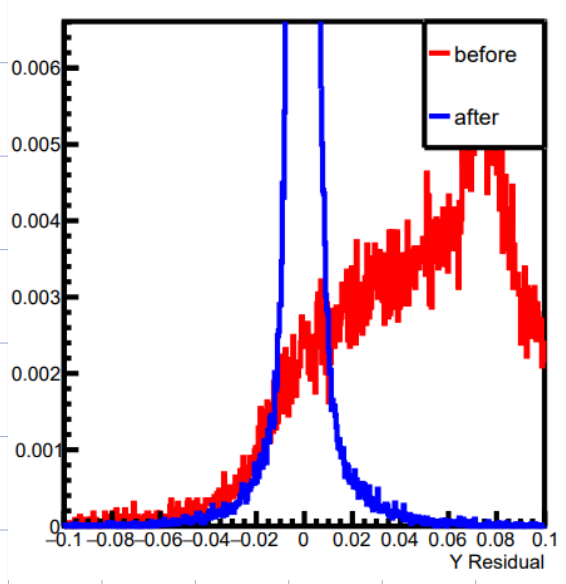
ResidualY Timepix3_2 before/after telescope Alignment



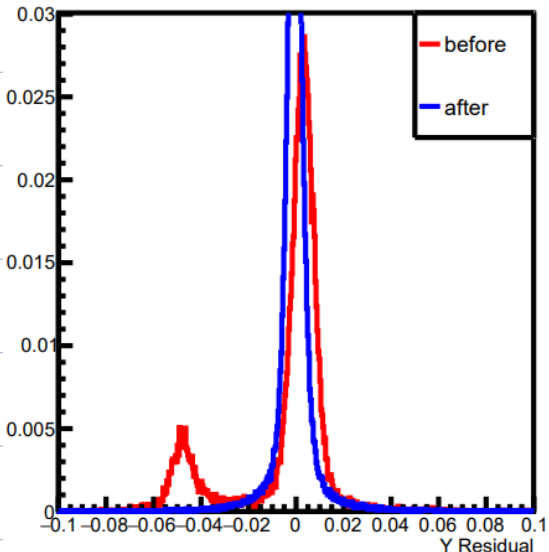
ResidualY Timepix3_3 before/after telescope Alignment



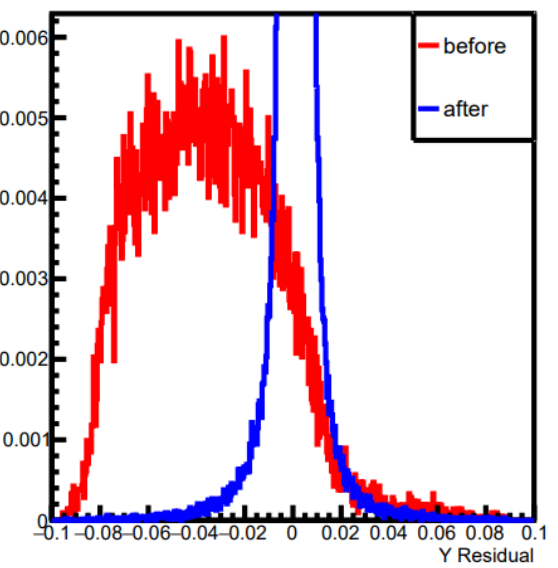
ResidualY Timepix3_4 before/after telescope Alignment



ResidualY Timepix3_5 before/after telescope Alignment

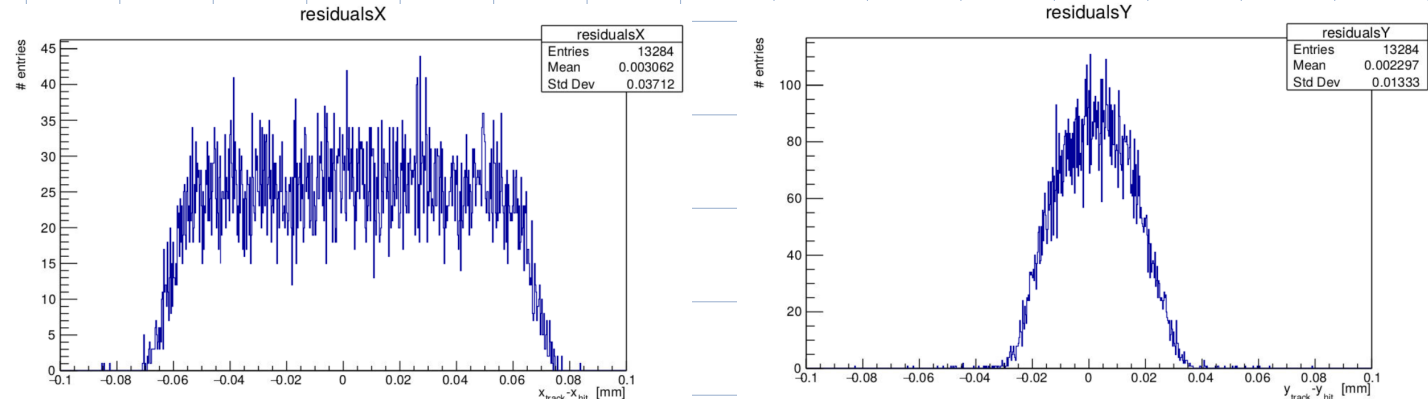


ResidualY Timepix3_6 before/after telescope Alignment



4.5.4 First DUT Residuals

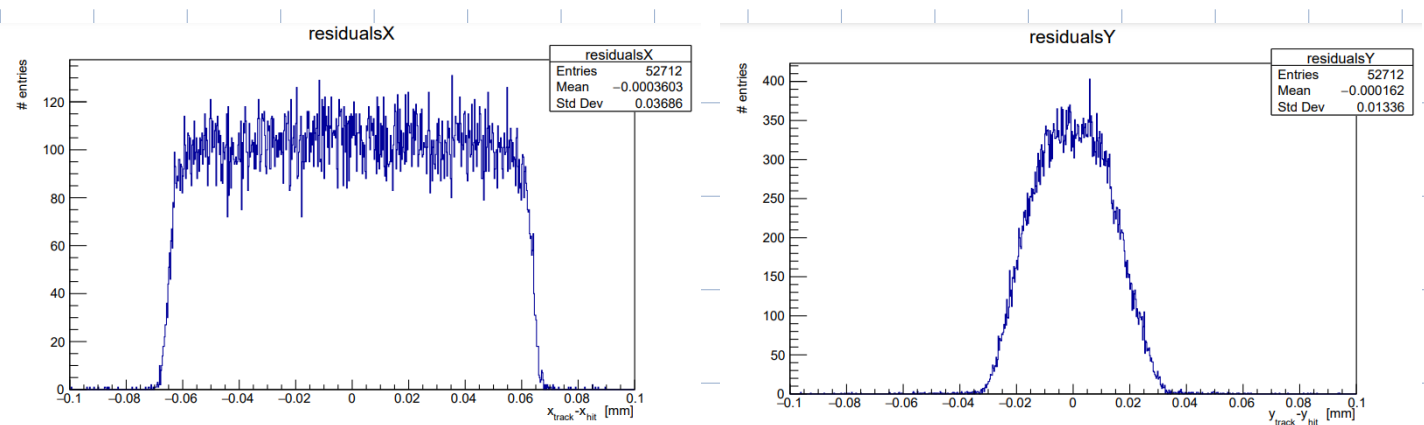
We add modules "AnalysisDUT" and "DUTAssociation" to associate the clusters on DUT to tracks and then calculate its residuals.



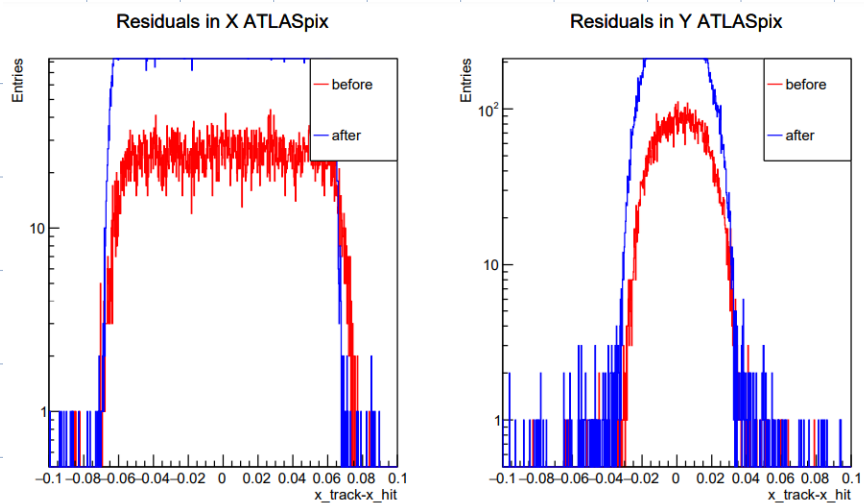
The DUT is excluded from tracking to ensure unbiased residuals and a reliable measure of its hit detection efficiency, because the hit-detection-efficiency of DUT is much smaller than the telescopes. Including the DUT in the track reconstruction could bias the residuals, resulting in false tracks that appear in the telescope but not in the DUT could be rejected. But by excluding it, we measure residuals that based only on the DUT's actual position relative to an independently reconstructed track from the reference telescope, so that any misalignment in the DUT can be prevented from distorting the tracking accuracy for other sensors.

4.5.5 DUT Alignment

We use module "Alignment DUT Residual" and run `09_alignment_dut.conf`, afterwards we get a new updated geometry file.



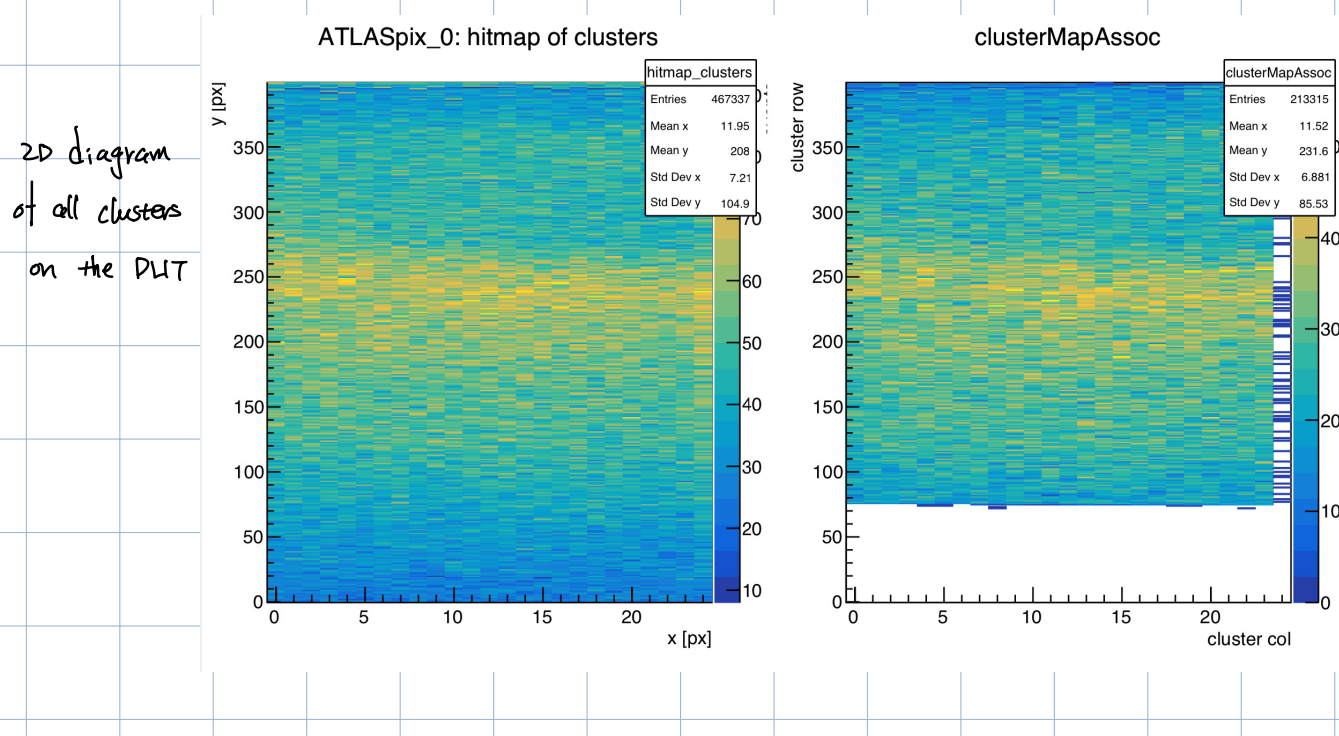
The mean of the two residuals are significantly reduced, below 1 km (10^{-3} mm).
The distributions are both symmetric. \Rightarrow precise alignment



The unbaised residuals are now centered and symmetric, signifying that the DUT position and rotation have been refined for optimal alignment with the reference setup.

4.6 DUT Analysis

We should analyse the entire data set and run the main configuration file 10-dut-analysis.conf

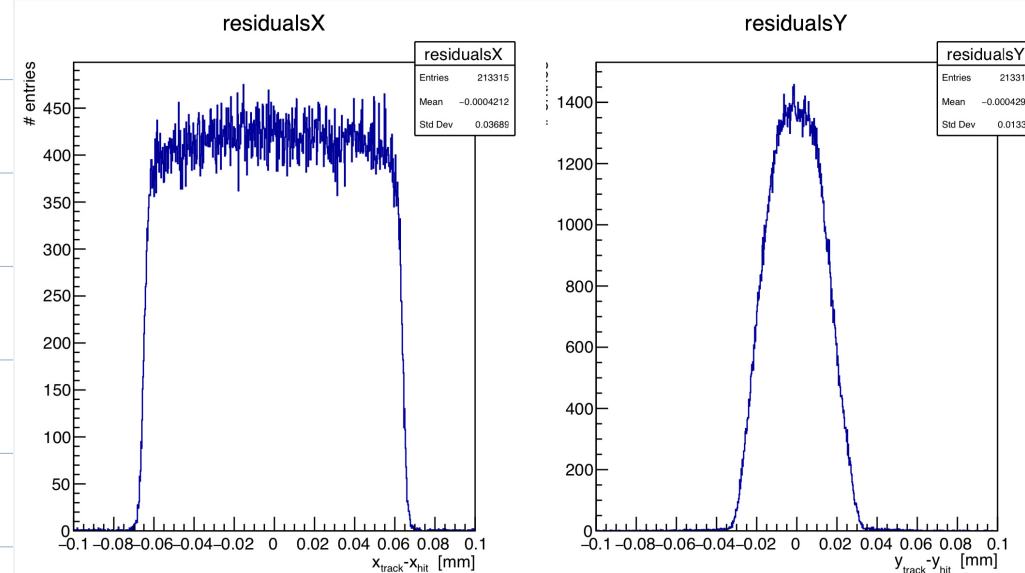


In the comparison of the histograms for the ATLASpix_0 bitmap of clusters and the clusters associated with tracks, we observe that the full matrix is not filled in the latter case. This difference can be attributed to the geometrical mismatch between the Timepix3 sensors in the reference telescope and the ATLASpix_Simple DUT. The ATLASpix_Simple sensor has a larger sensitive area than the Timepix3 sensors, meaning that not all clusters on the Timepix3 fall within the region observed by the DUT. As a result, only clusters within the overlapping region can be associated with tracks, leaving parts of the ATLASpix_Simple matrix unfilled in the associated cluster map.

4.6.1 Spatial Resolution

The width of the spatial residuals (RMS) can be used to estimate the spatial resolution.

$$\rightarrow \sqrt{\frac{\sum x_i^2}{n}}$$



- The residuals observed in `residualsX` and `residualsY` for the ATLASpix_Simple are **unbiased residuals**. This is because the DUT was excluded (as we can see in the configuration file) from the tracking, meaning the residuals are calculated between the track intercept and the cluster on the DUT without the cluster influencing the track fit, same as we got in 4.5.5.
- Quantification of the spatial resolutions of DUT: The spatial resolution is estimated from the RMS of the residuals, which is given as

$$\text{Root Mean Square (RMS)} = \sqrt{\frac{\sum x_i^2}{n}}$$

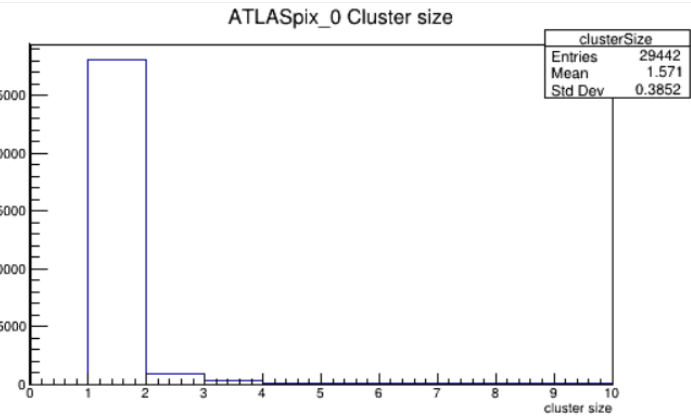
Since our mean value as zero can be settled to zero, the RMS is the Std. Dev.

- **X resolution:** 36.89 μm
- **Y resolution:** 13.36 μm

- The spatial resolutions are **reasonable** but are higher than the ideal "binary resolution" for the ATLASpix_Simple sensor (37.53 μm in x and 11.55 μm in y). Based on Equation (5) in Section 3, the expected binary resolution is approximately

$$RMS_{\text{binary}, x/y} = \frac{\text{pixel pitch in } x/y}{\sqrt{12}}$$

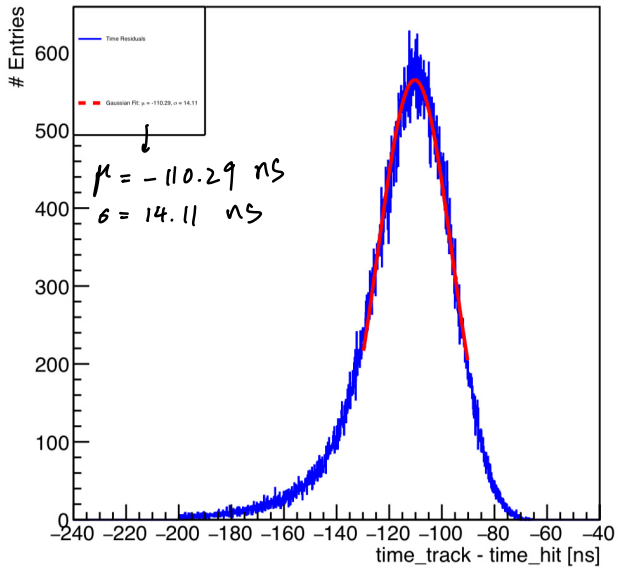
Since the binary resolution shows us that for pixel sensors with little or no charge sharing, in other word, mostly clusters of size 1. so if we observe the cluster size distribution of ATLAS_simple, we found that the most clusters on the DUT are 1-pixel-clusters. Therefore we would expect the resolution to be closer to this value. The slight deviation from the binary resolution can be resulted in factors like the precision limit of the reference telescope.



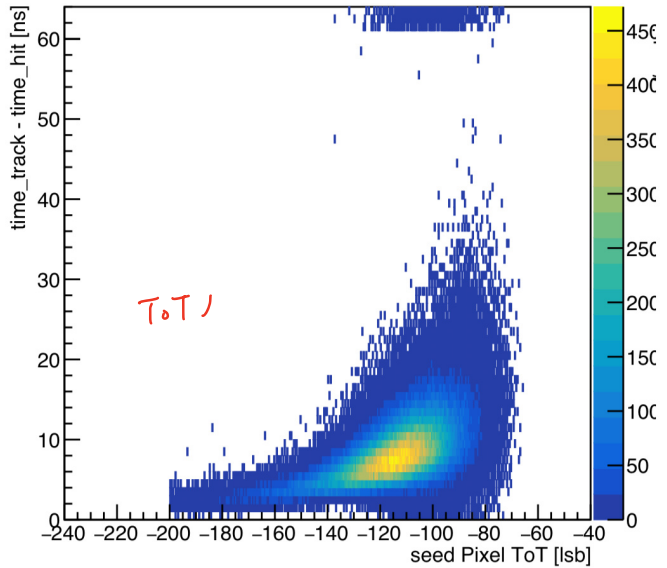
- The spatial residuals are non-Gaussian likely due to the relatively large pixel size of the ATLASpix_Simple 130 $\mu\text{m} \times 40\mu\text{m}$ compared to the telescope's precision 55 $\mu\text{m} \times 55\mu\text{m}$. With a coarse pixel size, the sensor's resolution is limited, causing discrete residual values based on pixel size rather than a smooth distribution. This **pixelation effect**, combined with minimal charge sharing (binary resolution bigger so that the width broader), leads to the non-Gaussian shape in the residuals distribution.

4.6.2 Time Resolution

ATLASpix Simple Time Residuals



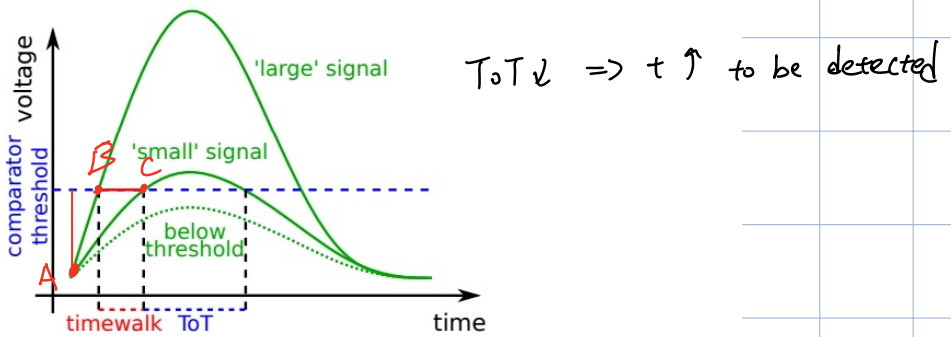
Time Residuals vs ToT



- ATLASpix Simple Time Residuals: A histogram displaying the distribution of time residuals between the reference tracks and the associated clusters on the DUT, with a Gaussian fit applied.
- Time Residuals vs ToT: A 2D histogram plotting the same time residuals as in the first plot versus the Time-over-Threshold (ToT) of the seed pixel in the cluster, which shows a spread of residuals as ToT decreases (for the value of ToT we only consider its absolute value).

$$t_{\text{residual}} = t_{\text{track intercept}} - t_{\text{associated cluster}}$$

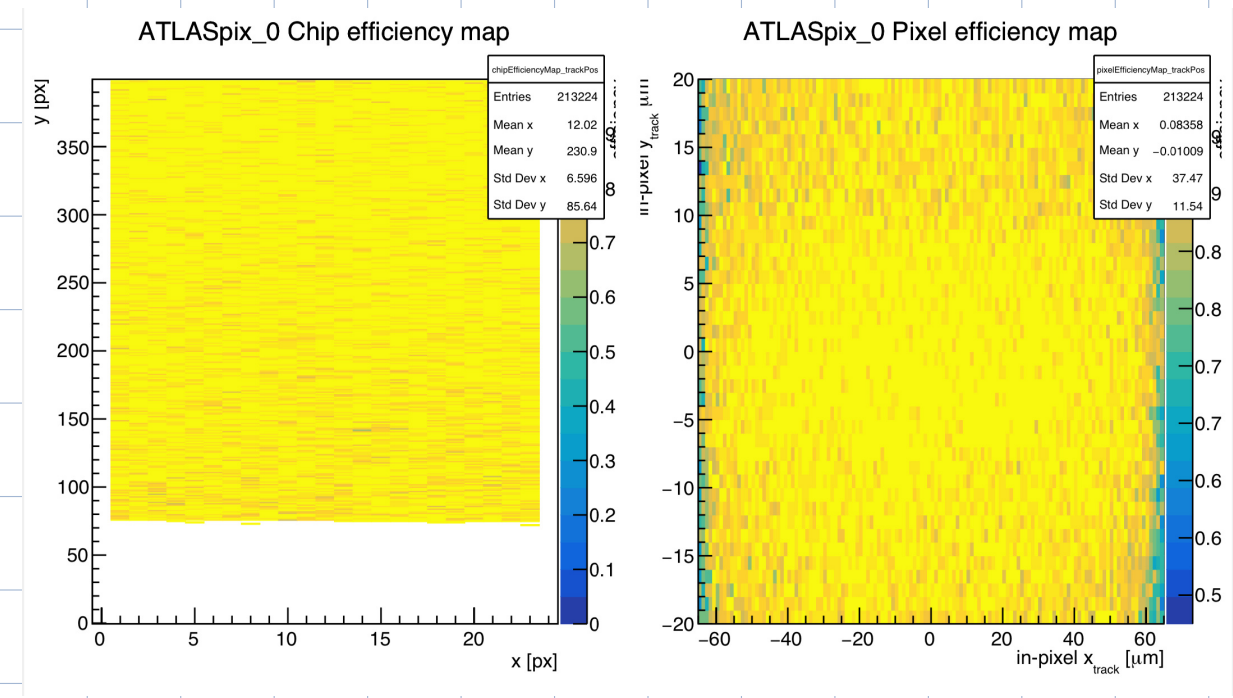
- The offset from zero (mean value μ) can affect the interpretation of the time resolution, as it indicates a systematic timing shift. This offset could be caused by delays in signal processing. As we found in the time diagram under, a particle track hit on the detector at t_{track} in point A and induced a „visual“ signal, this signal takes time to be detected in B at a later timestamp t_{hit} . So there is a nonzero offset between A and B, for the small signal with lower ToT, the time interval to be detected will increase.



- The distribution in the time residual histogram shows a strong **non-Gaussian tail**, likely due to **timewalk**. Timewalk occurs because smaller signals (lower ToT) take longer to reach the detection threshold, leading to delayed timestamps relative to larger signals. This results in a tail, which matches the data as seen in the histogram. The 2D histogram confirms this by showing a clear correlation between lower ToT values and higher time residuals (time interval between B and C), which visualizes the impact of timewalk.
- We can get the time resolution also from the RMS of the residual distribution namely the standard deviation.
 - Time resolution from Std. Dev. without Gauss fit: 17,66 ns
 - Time resolution from Gauss fit: 14,11 ns

However, since the distribution has a strong tail, the RMS of the entire distribution (not just the Gaussian core) might be a better measure for the overall time resolution.

4.6.3 Hit Detection Efficiency



- The hit detection efficiency is derived from the probability of detecting particles as they pass through the sensor.

$$\epsilon = \frac{\text{\# tracks with an associated cluster}}{\text{\# tracks with + without an associated cluster}}$$

From the Chip efficiency map, we see values close to 1 in much of the map, indicating a high detection efficiency across the chip.

- We think that the chip efficiency map may not be fully filled, because as we can see in the plot of associated clusters on the DUT at the beginning of section 4.6, the number of associated clusters at the bottom of the „clusterMapAssoc“ is zero. And certain pixels might not detect hits due to hardware defects or lack of connectivity.
- The pixel efficiency map has the highest efficiency in the middle and around the edges the efficiency becomes lower. As particles passing through the center are fully captured, while those near edges might be less likely to trigger a full detection. The lower efficiency at the pixel boundaries can occur if charge sharing affects the detection threshold, leading to lower detection efficiency near edges compared to the center.

Reference

Jens Kröger, script F96 Characterisation of Silicon Pixel Sensors for High-Energy Physics, Version 1.0.2 (July 6, 2020), Ruprecht-Karls-Universität Heidelberg.
<https://www.physi.uni-heidelberg.de/Einrichtungen/FP/anleitungen/F96.pdf>